Overview of observational methods and instruments: spectrographs

Sergei Shestov


DARK SIDE
OF THE
MOON

Outline

- Scientific importance of spectroscopic observations
- Solar spectra
- Methods & assumptions of spectroscopic analysis
- Layout of a generic spectrograph
- Types of spectrographs:
  - Slit spectrograph
  - Slitless spectrographs
  - Crystal spectrographs
  - Photometers
  - Solid state spectrographs
- Literature

Some facts about spectroscopic observations

- Bohr's model of the Hydrogen atom (1913);
- Hubble's law (1927, based on V. Splipher redshifts);

- Solar corona: determination of temperature (Edlen, 1942), chemical composition;
- Atomic physics: atomic structure (di-el. satellites), precise energy levels (the IRON project)

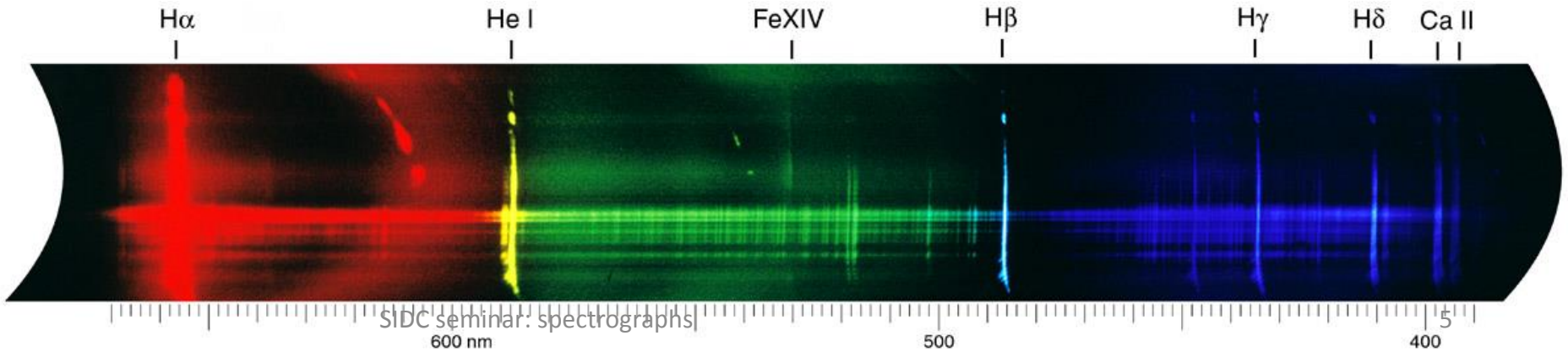

Solar corona spectrum

- Black-body T=5762 K in white-light (thermodynamic eq.);
- Charged ions emit spectral lines and continuum as a result of excitation;
- Bremsstrahlung emission of electrons;

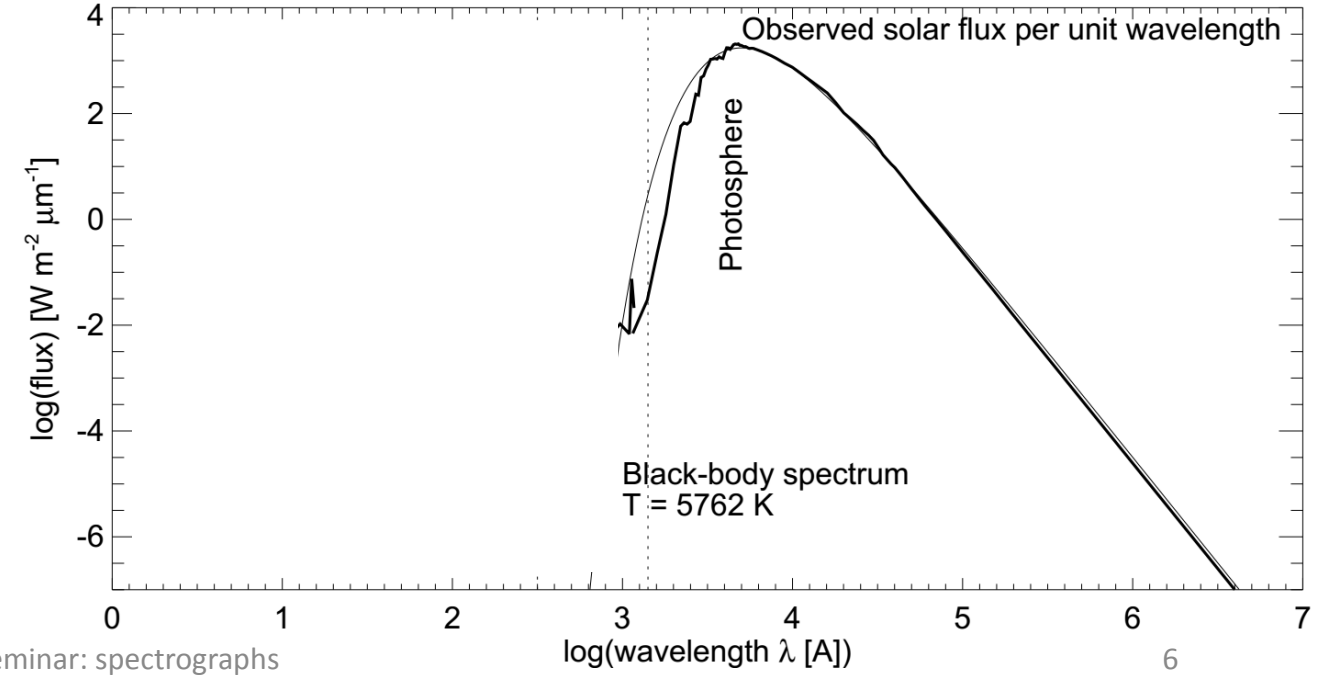

Bohr atom model, H-like atoms

$$\frac{1}{\lambda} = \frac{\nu}{c} = \frac{Z^2 m e^4}{4\pi\hbar^3 c}\left[\frac{1}{n_f^2} - \frac{1}{n_i^2}\right]$$

H	Z=1	~ 1215 Å
He II	Z=2	~ 304 Å
…		
Mg XII	Z=12	~ 8.42 Å
…		
Fe XXVI	Z=26	~ 1.80 Å

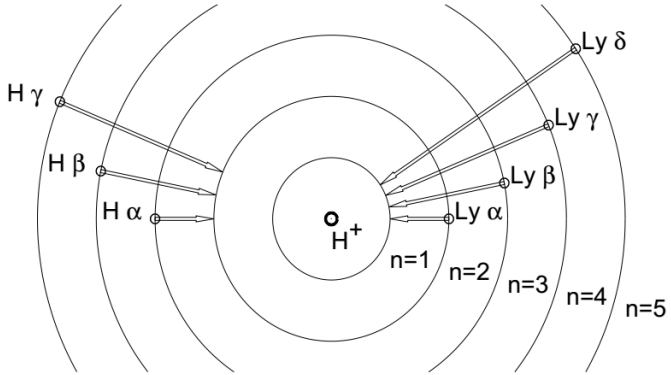

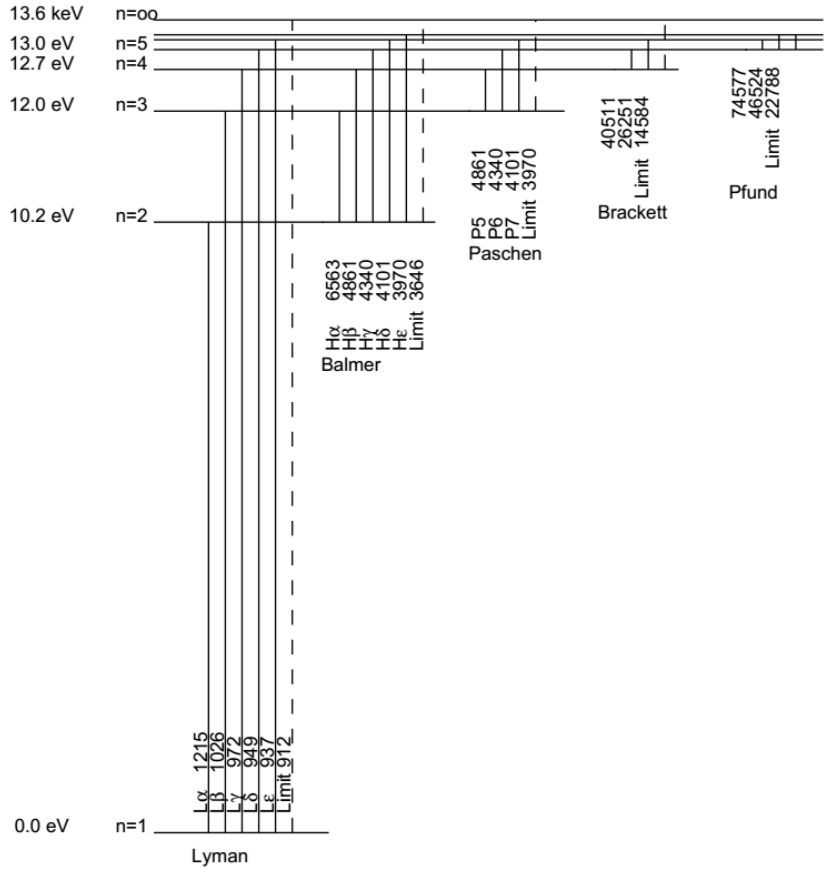

Fe IX 170.07 Å: $3p^6\ {}^1S_0$ <- $3p^5 3d\ {}^1P_1$;

Fe XII 195.12 Å: $3s^2\ 3p^3\ {}^4S_{3/2}$ <- $3s^2\ 3p^2\ (3p)\ 3d\ {}^4P_{5/2}$

Methods of spectroscopic analysis

$$I_{h\nu} \sim N^{j}_{X,+m} \cdot A_{ji}$$

$$N^{j}_{X,+m} \sim N^{g}_{X,+m} \cdot N_e \sim Ab_X \cdot f(T, n_e)\, N_H N_e$$

$$I_{h\nu} \sim Ab_X \cdot f(T, n_e) A_{ji} \cdot N_H N_e$$

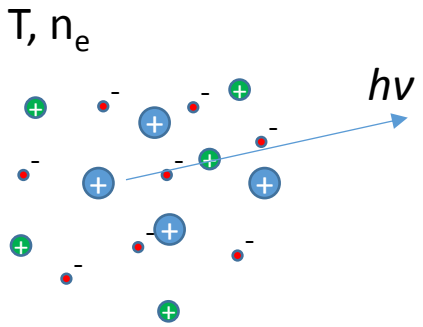

- Intensities of individual lines – distribution of T, n_e;
- Spectral line shape – T, presence of flows;

Necessary simplifications

$I_{h\nu} \sim Ab_X \cdot f(T, n_e) A_{ji} \cdot N_H N_e$

- Optically thin
- Ionization equilibria
- Electron excitation are more frequent

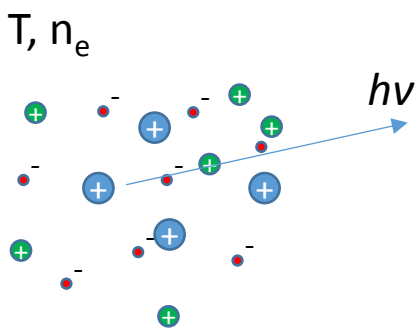

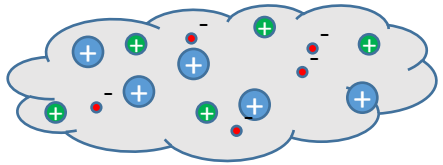

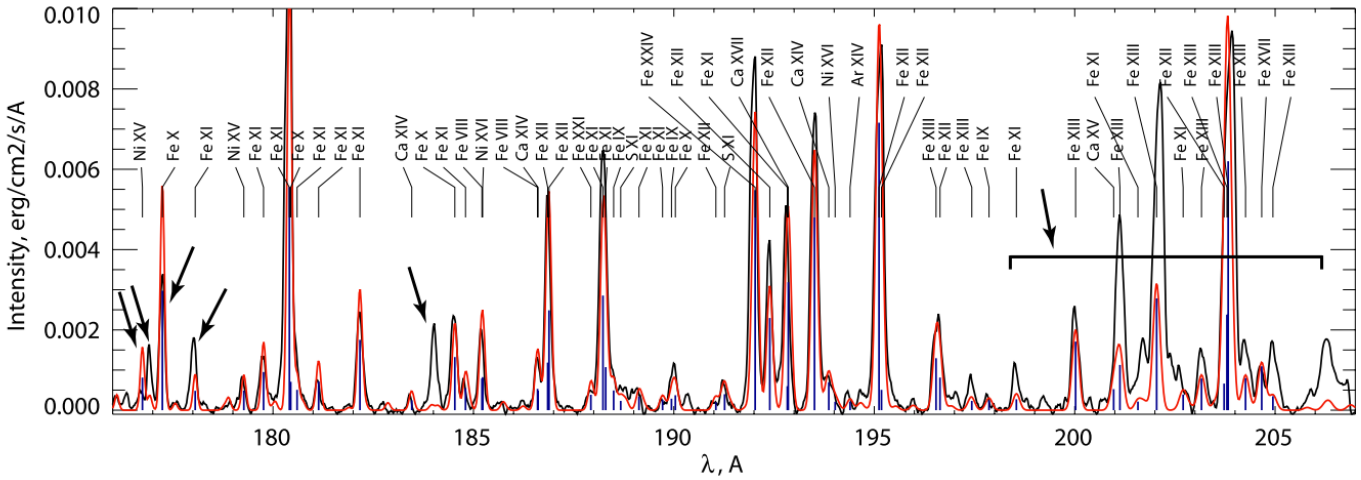

Necessary simplifications

$I_{h\nu} \sim Ab_X \cdot f(T, n_e) A_{ji} \cdot N_H N_e$

- Optically thin
- Ionization equilibria
- Electron excitation are more frequent

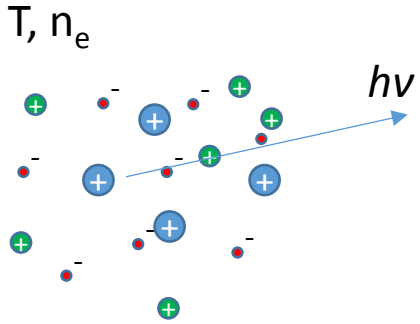

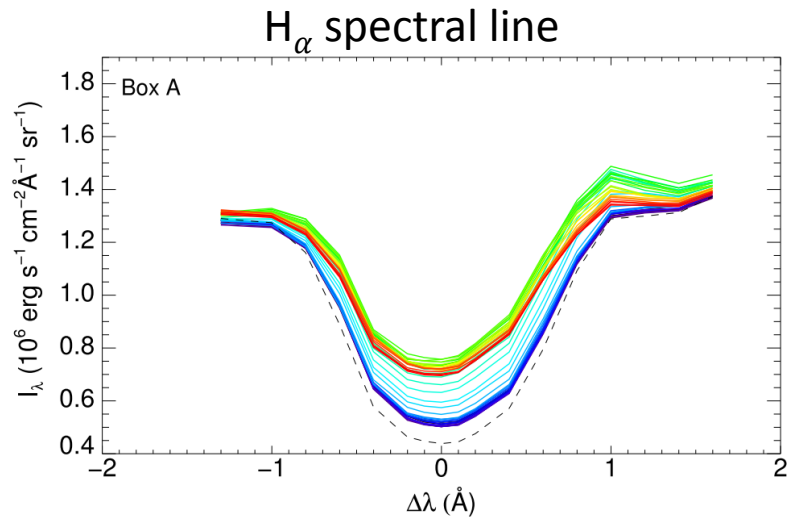

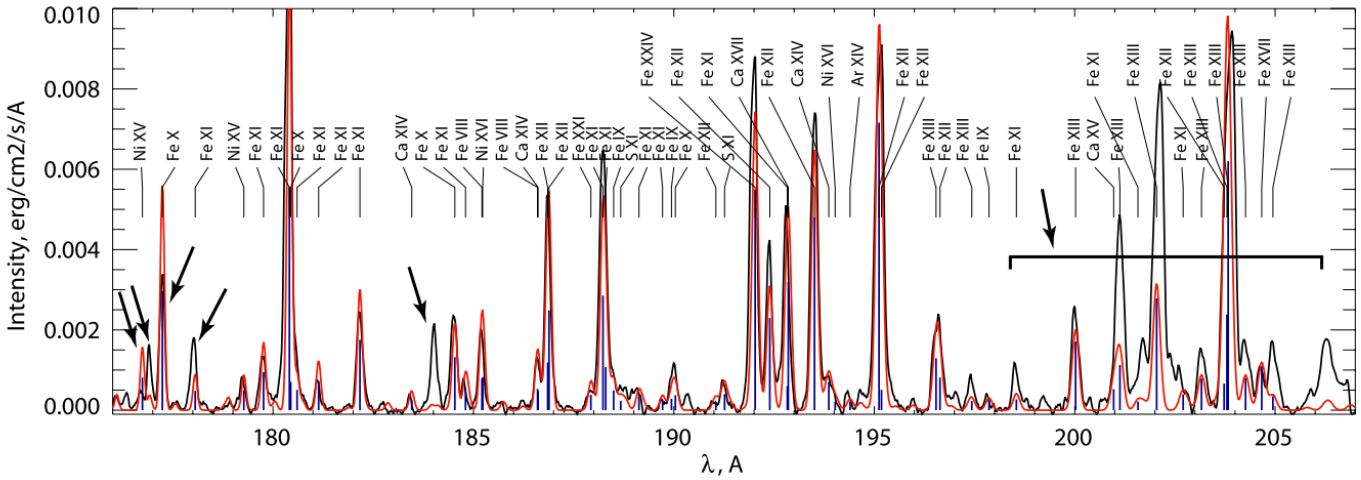

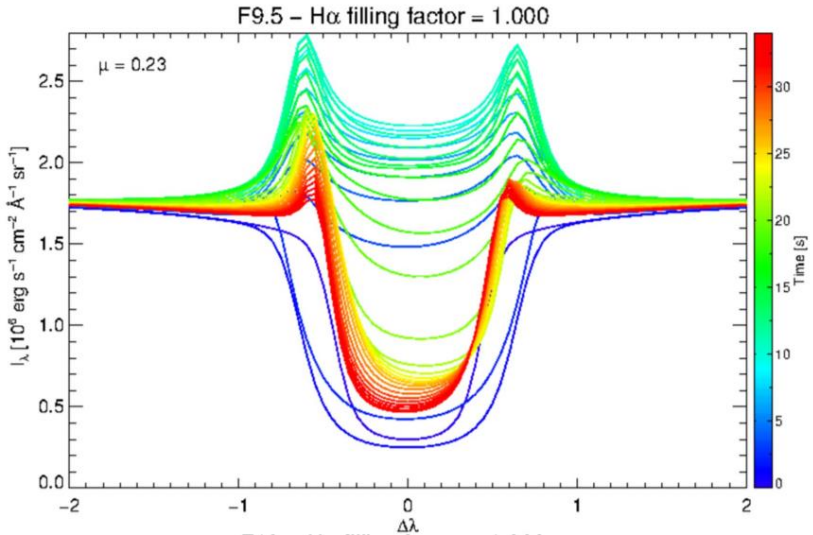

Generic layout of a spectrograph

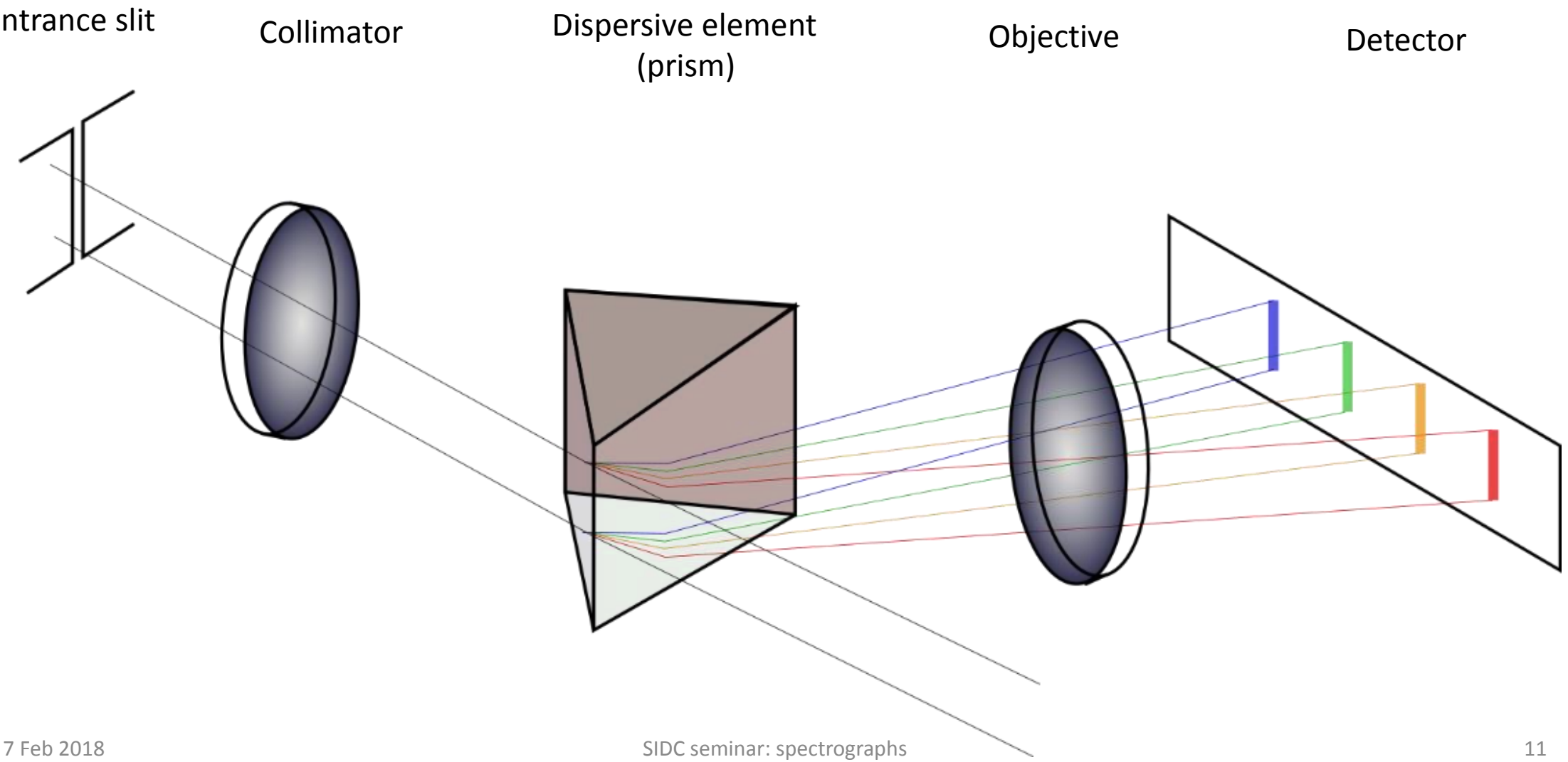

Types of spectrograph

- Diffraction grating based
  - Slit
    - down to 30 Å;
    - EIS/Hinode; CDS, SUMER (SOHO); SERTS; VAULT; IRIS
  - Slitless
    - Skylab S082A; SPIRIT/CORONAS-F; EVE/SDO;
- Photometers
  - 1-2500 Å;
  - Lyra/PROBA-2; GOES SXR;
- Crystal based
  - 0.5 – 30 Å;
  - RESIK, DIOGENESS, Mg XII (CORONAS-F); BCS, FCS (SMM); BCS/Yohkoh;
- Solid state based
  - Si – 0.5-15 keV (0.8-30 Å); Ge – 4 keV-17 MeV;
  - SphinX/CORONAS-PHOTON; RHESSI; SOXT;

Slit spectrograph – EUV & UV spectral range

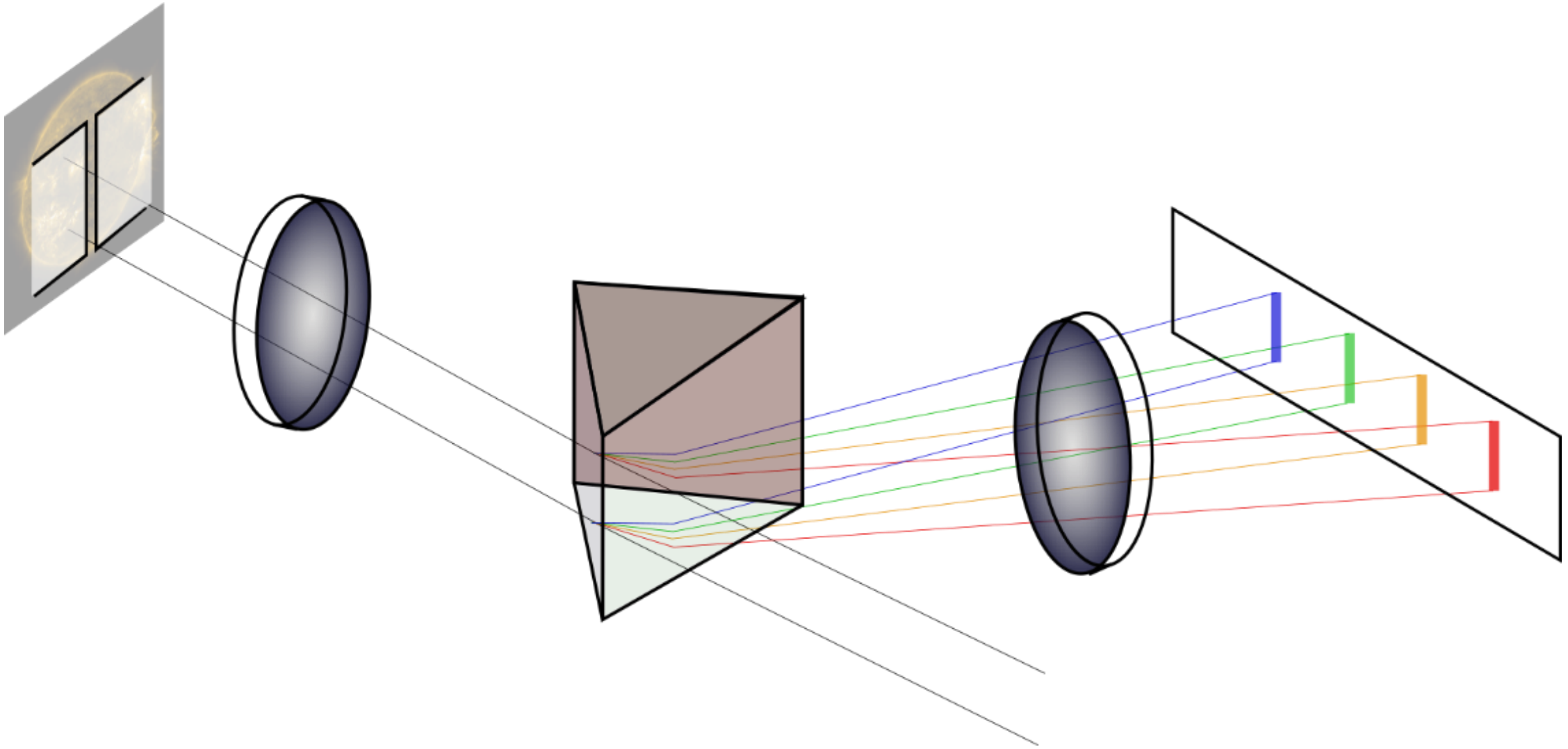

IRIS UV spectrograph

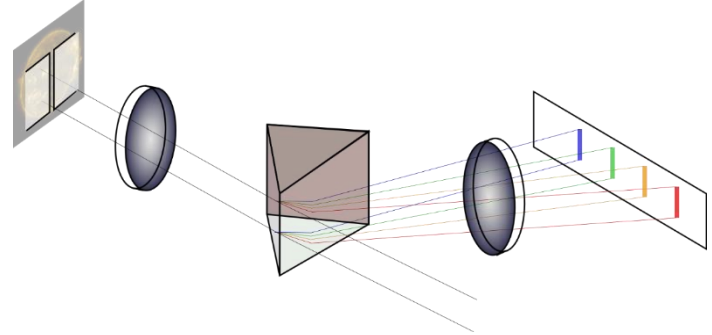

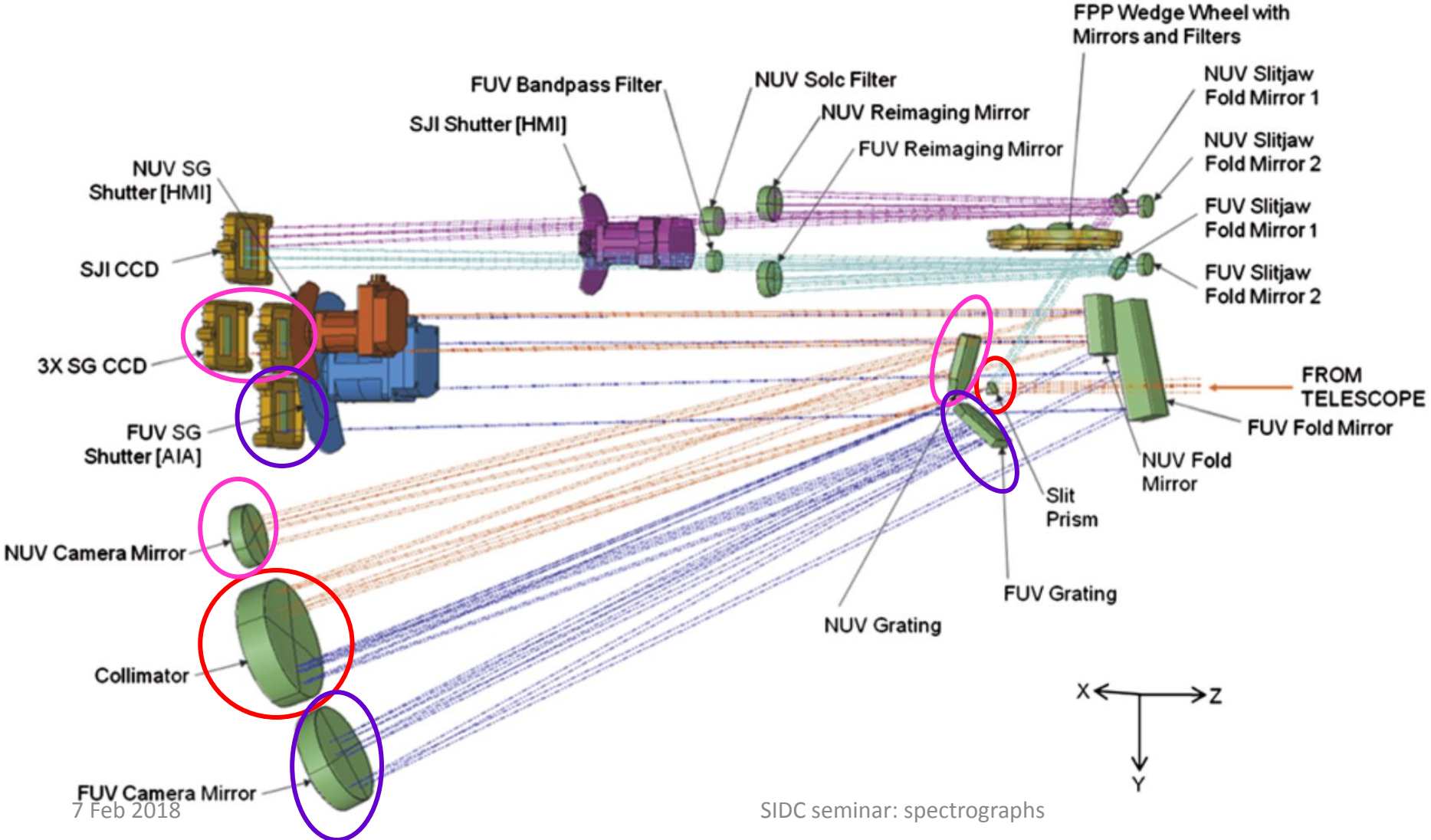

- SUMER/SOHO – 390-1610 Å
- CDS/SOHO – 150-800 Å
- EIS/Hinode – 170-210, 250-290 Å
- IRIS – 1330-1360, 1390-1410, 2780-2850 Å
- SERTS – 170-225, 235-450 Å
- SPICE/Sol.Orb. – 704-790, 970-1040 Å

Fe XII 195.12 Å from EIS/Hinode

Monochromatic image

Doppler shift map

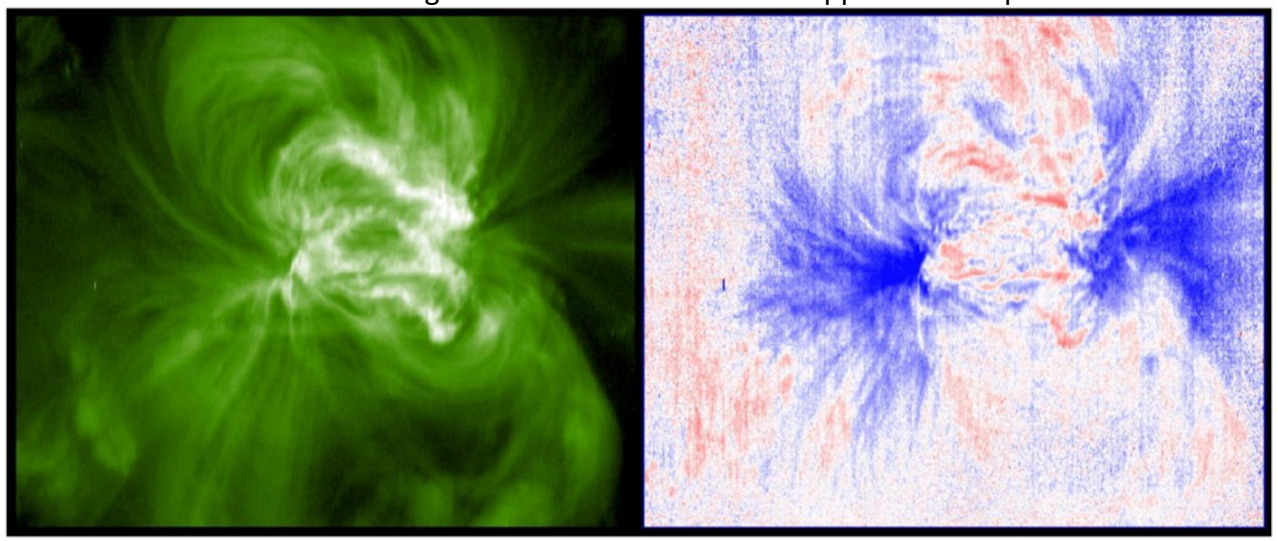

FUV spectra from IRIS (Tian et al. 2015)

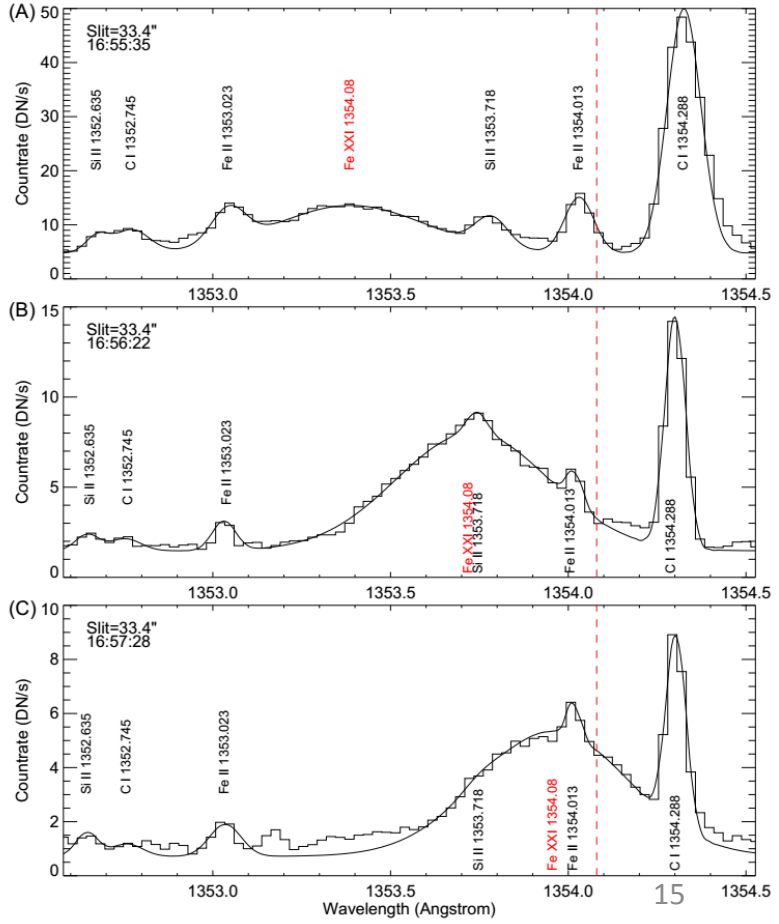

Pros & Cons – slit spectrographs

- High spectral resolution & spatial resolution in □ direction;
- Spectra of small regions covered by the slit or slot;

- Impossible to get simultaneous spectra of the whole Sun – scanning;
- Large amount of optics – small sensitivity;

Save the ~~whales~~ photons!

Spectroheliograph – EUV & UV spectral range

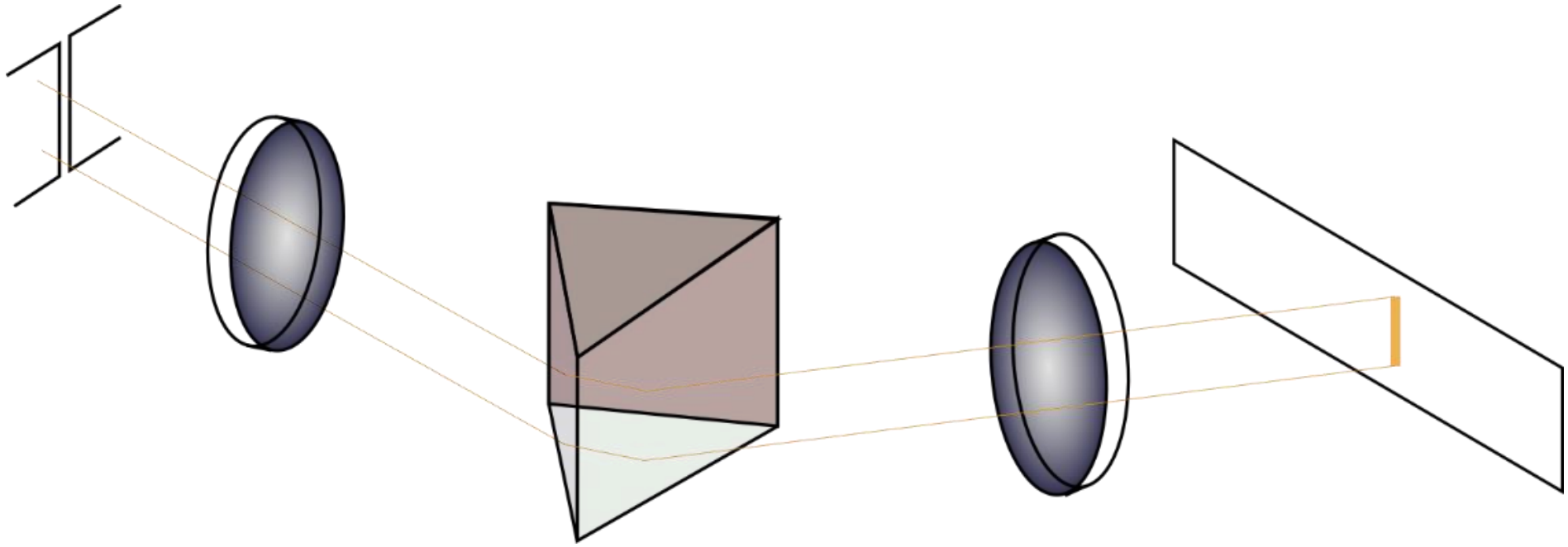

Spectroheliograph – EUV & UV spectral range

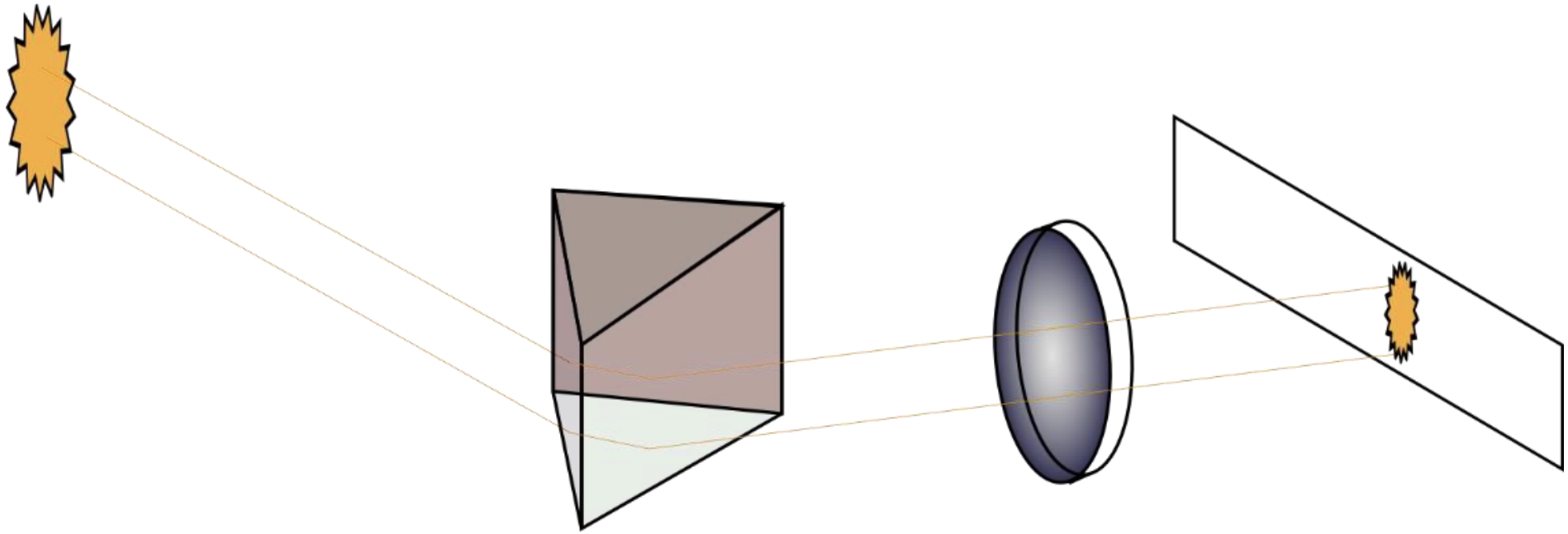

Spectroheliograph – EUV & UV spectral range

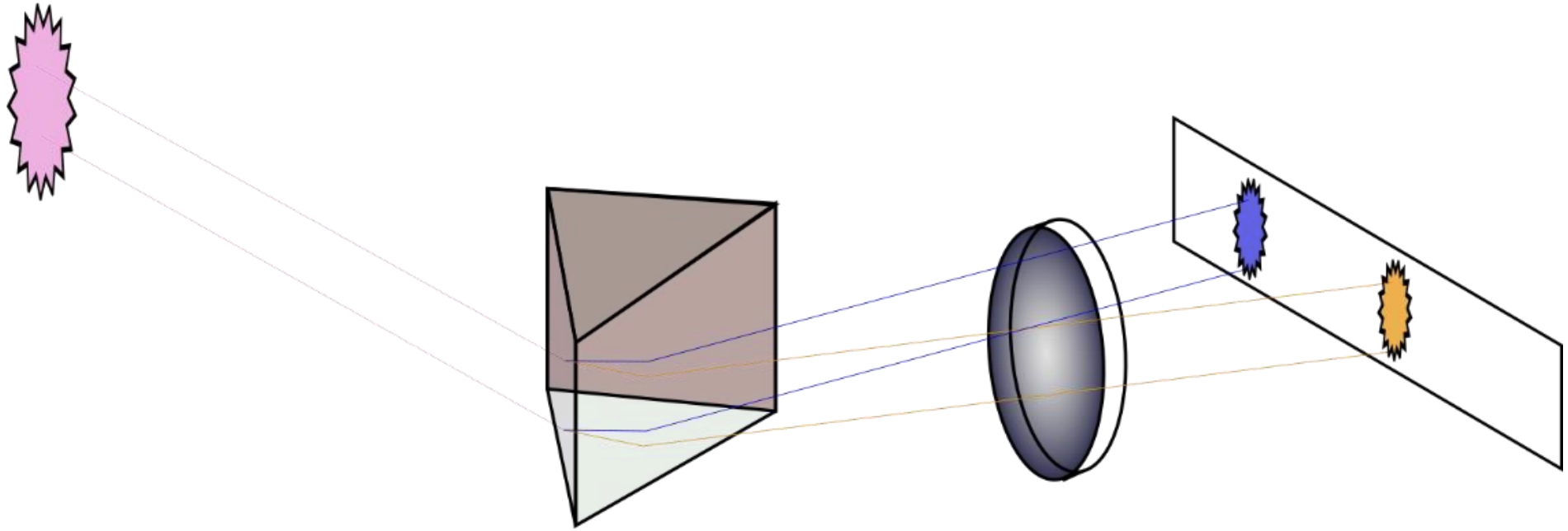

S082A spectroheliograph on Skylab

- 170-630 A;
- Concave grating;
- Photographic film;

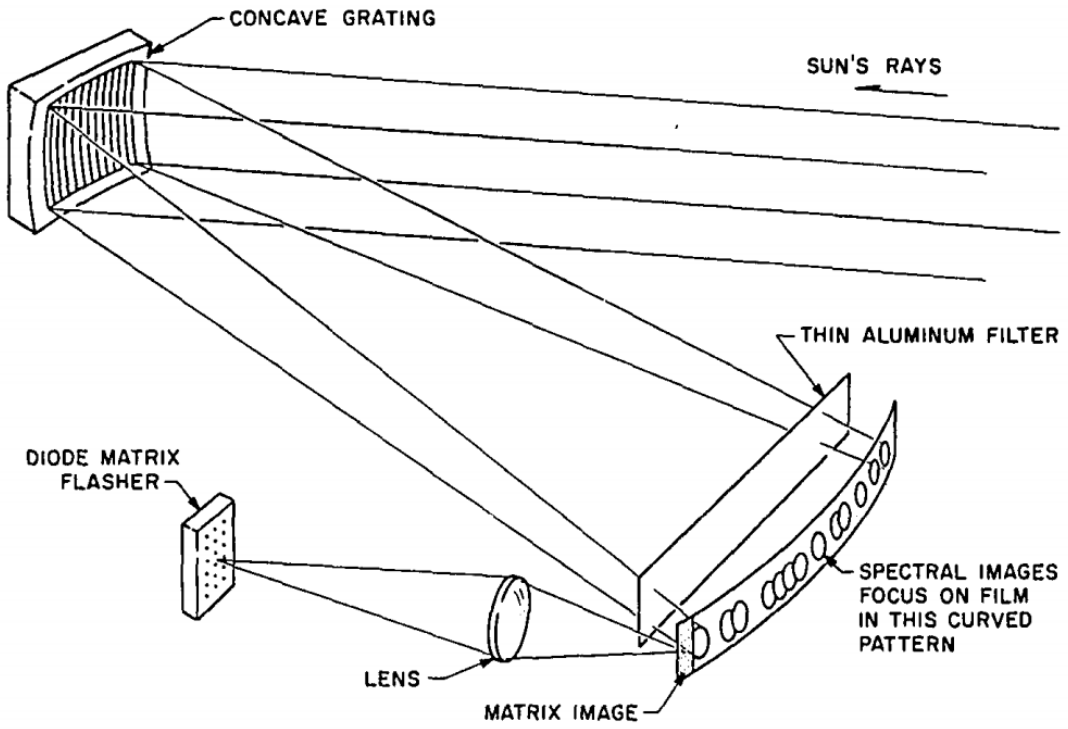

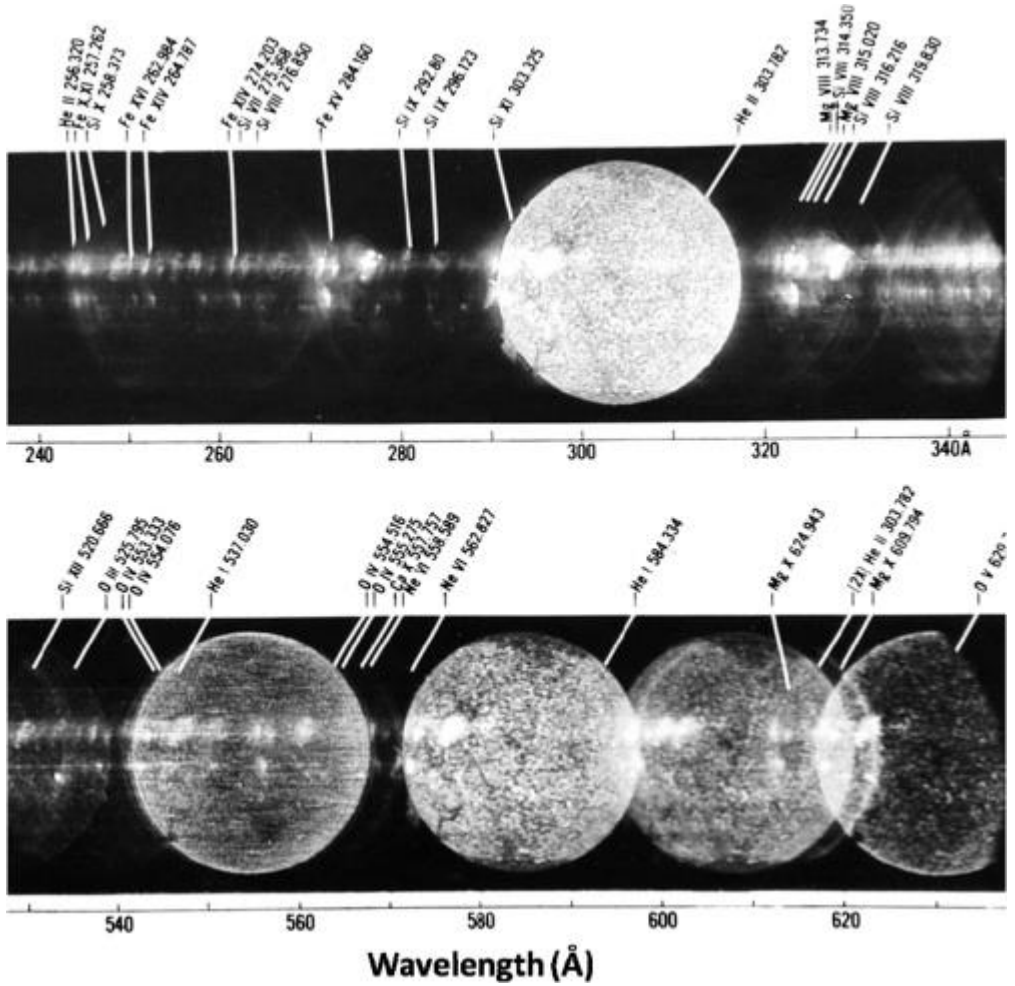

SPIRIT EUV spectoheliograph on CORONAS-F

- 176-207, 280-335 A;
- Plane grating, grazing incidence;
- Multilayer mirror & CCD-based detector

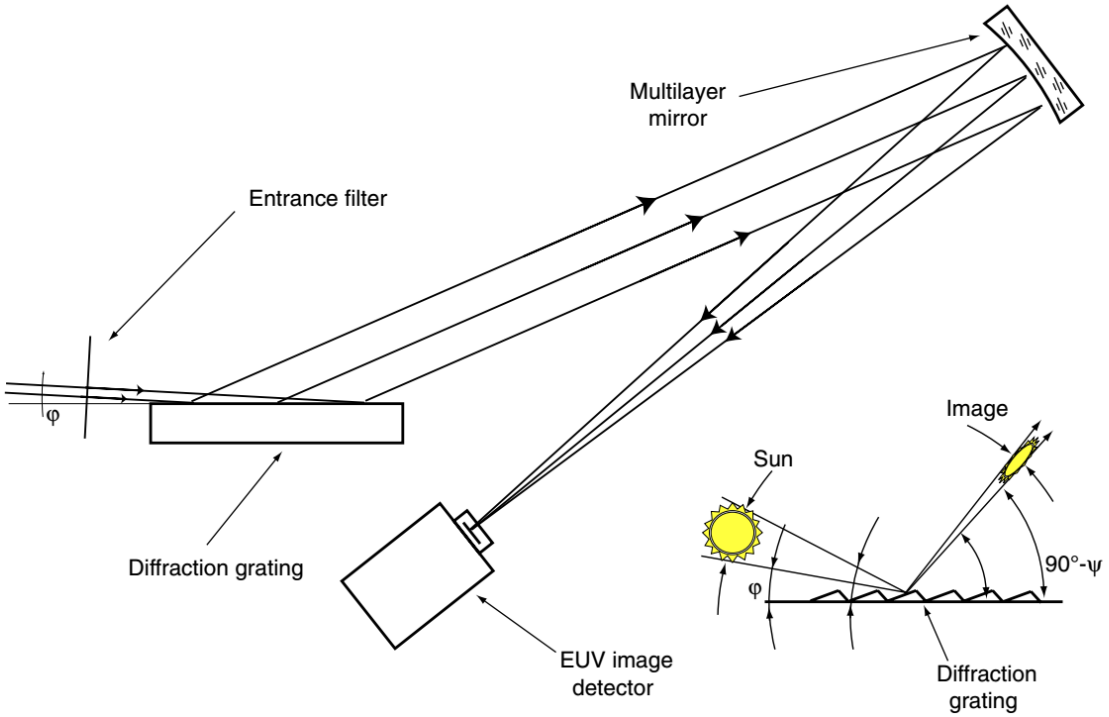

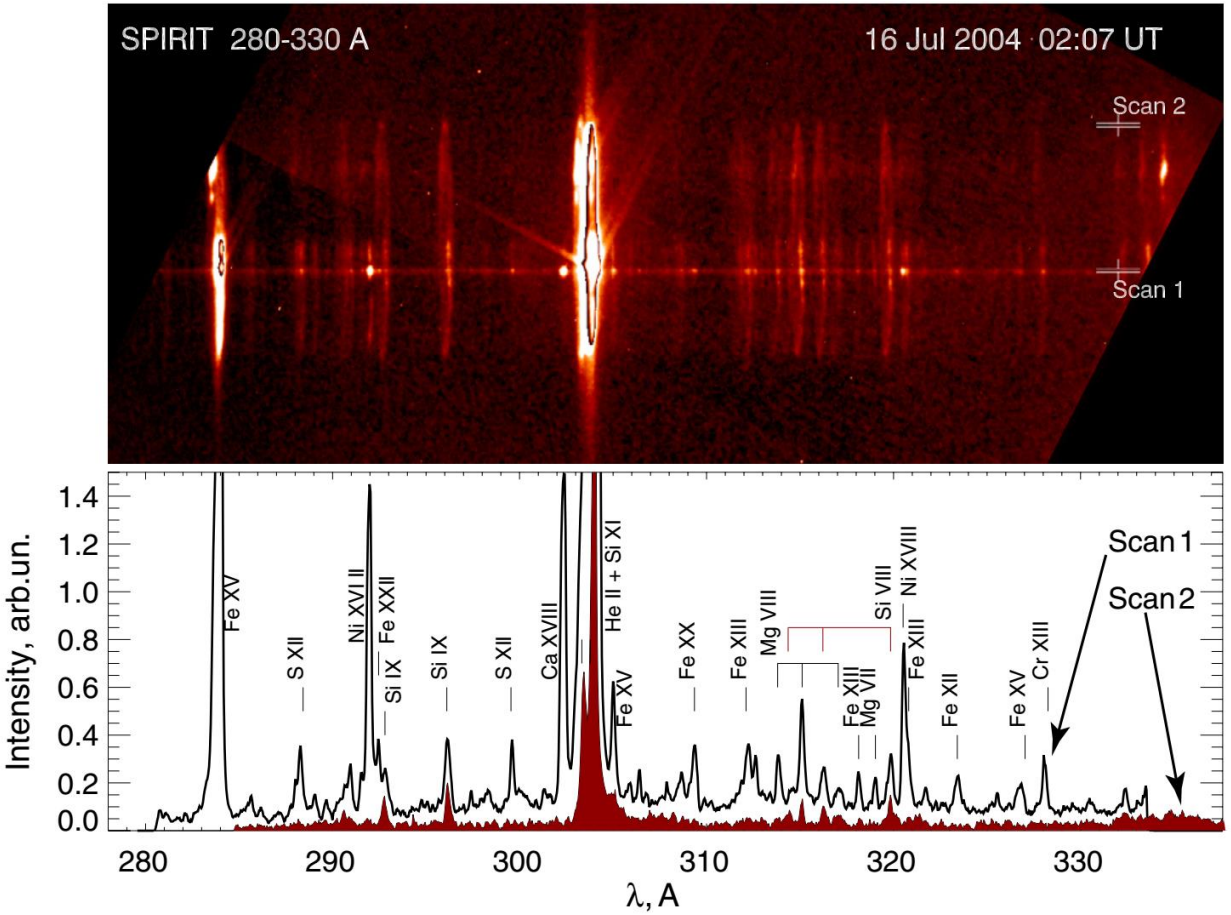

Pros & Cons – spectroheliographs

- Full-Sun spectral images;
- Higher sensitivity ?
- Possibility for high corona observations;

- Lower spatial resolution WRT slit spectrographs;
- Monochromatic images are overlapping – overlapograms;
- Difficult to analyze data;

Future: **COSIE** for the ISS – CfA, for the high corona observations
KORTES for the ISS – LPI, studying of flaring plasma

EUV slit spectrograph with no imaging – EVE/SDO

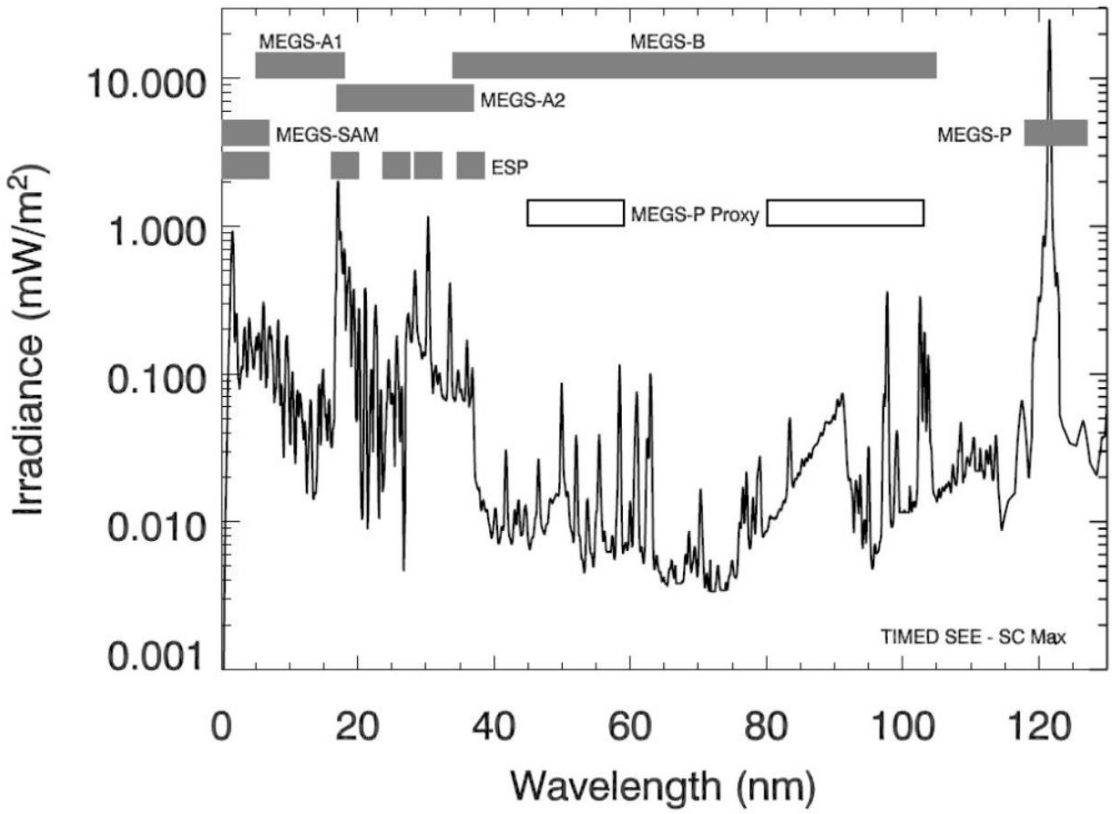

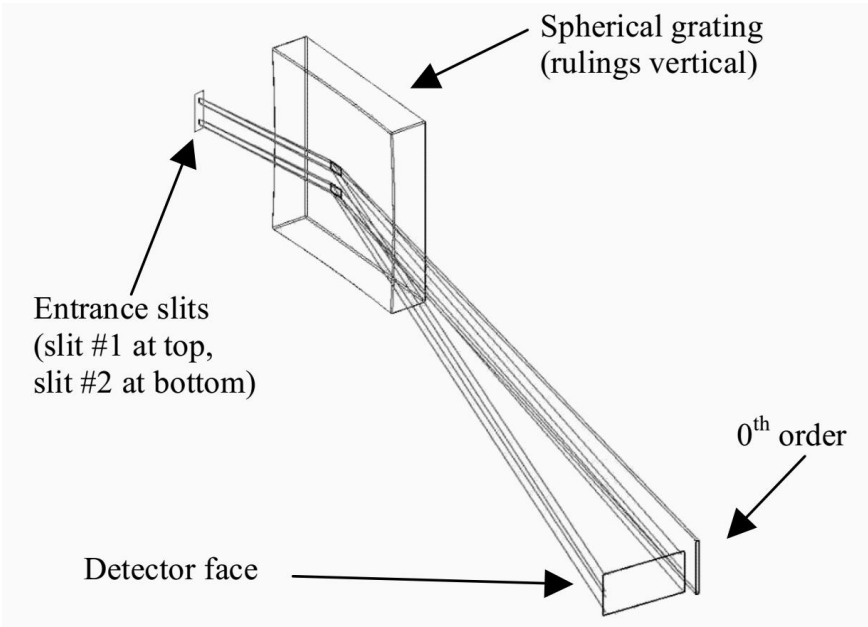

EUV slit spectrograph with no imaging – EVE/SDO

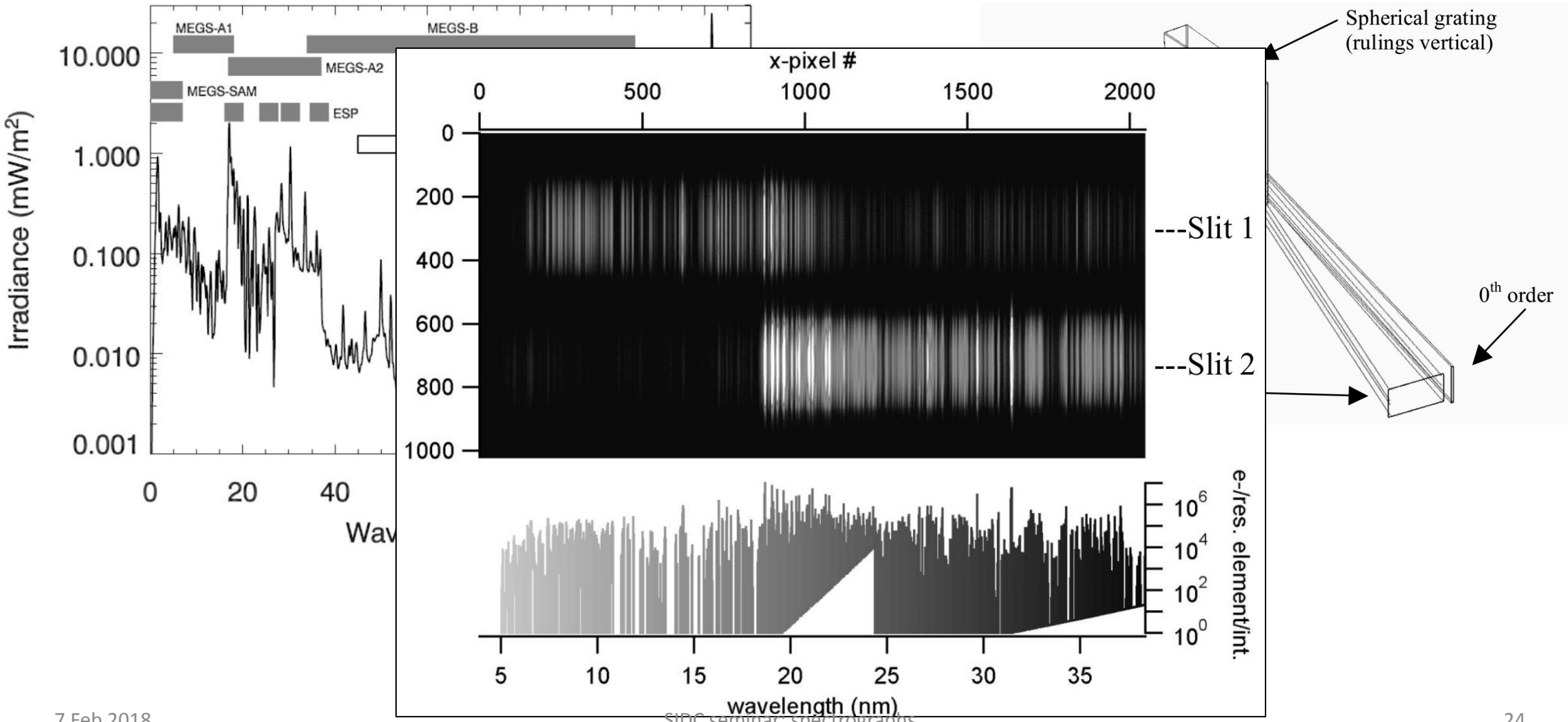

Pros & Cons

- No spatial resolution – average spectrum of the Sun;
- Very wide spectral bandwidth;
- High temporal resolution;
- High sensitivity;

Crystal spectrograph

- Low λ – impossible (almost) to use diffraction gratings;
- Crystals – Bragg-Wulf law:

$$n\lambda = 2d \sin \lambda$$

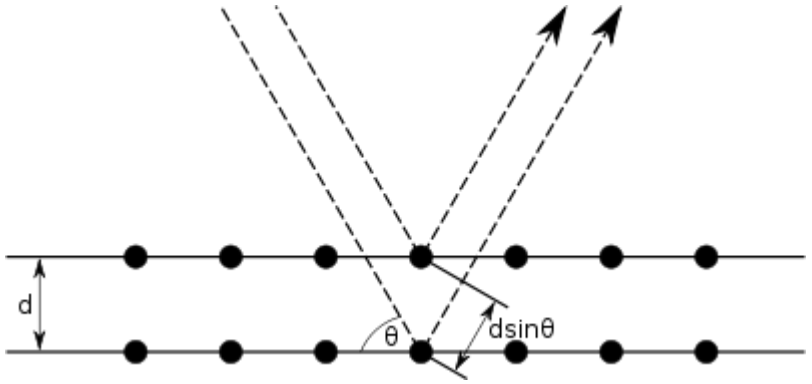

Crystal spectrograph

- Low λ – impossible (almost) to
- Crystals – Bragg-Wulf law:

$$n\lambda = 2d \sin \lambda$$

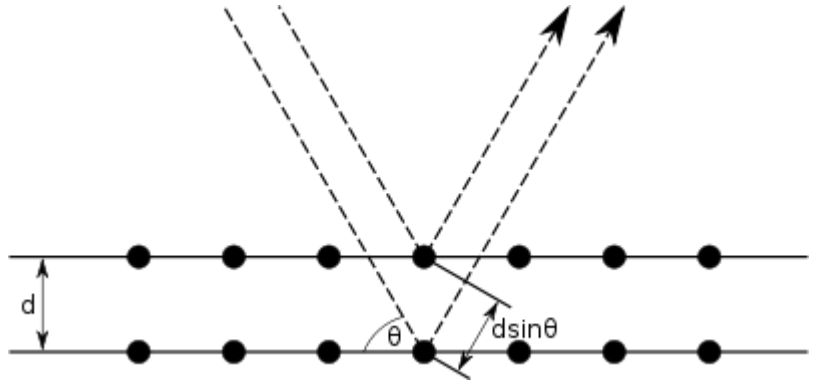

Mission	Instrument	Spectral range, A	Crystal
Solar Maximum Mission	BCS	1.769-1.796	Ge 422
	Bent crystal spectrometer	3.165-3.231	Ge 220
	FCS		
CORONAS-F	DIOGENESS	3.14-3.39	Quartz 101
		4.98-5.37	ADP
		6.11-6.73	Beryl
		2.96-3.21	Quartz 10-10
	RESIK	3.40-3.80	Si 111
		4.35-4.86	Quartz 10-10
Yohkoh	BCS	1.76-1.80	Ge 222
	Bragg crustal spectrometer	1.83-1.89	Ge 222
		5.02-5.11	Ge 111
Hinotori			
Intercosmos			
P78			

Flat and Bent-crystal spectrographs

BCS/Yohkoh (1991-2001)

1.7-5.1 Å

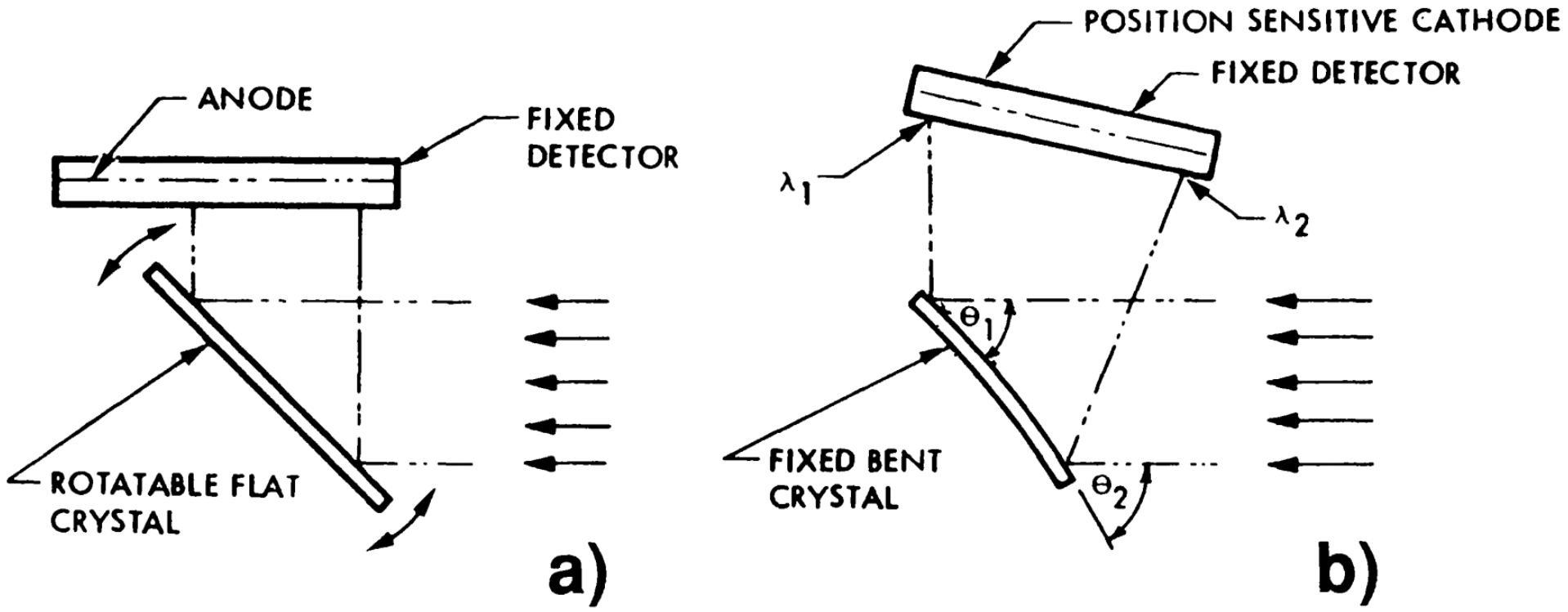

RESIK flare spectra

RESIK/CORONAS-F (2001-2005)

3.5 – 6.1 Å

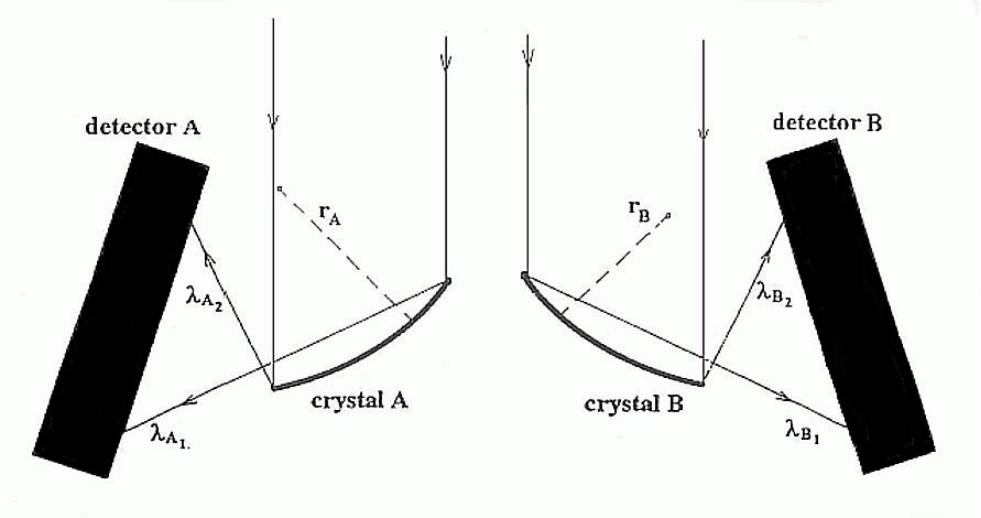

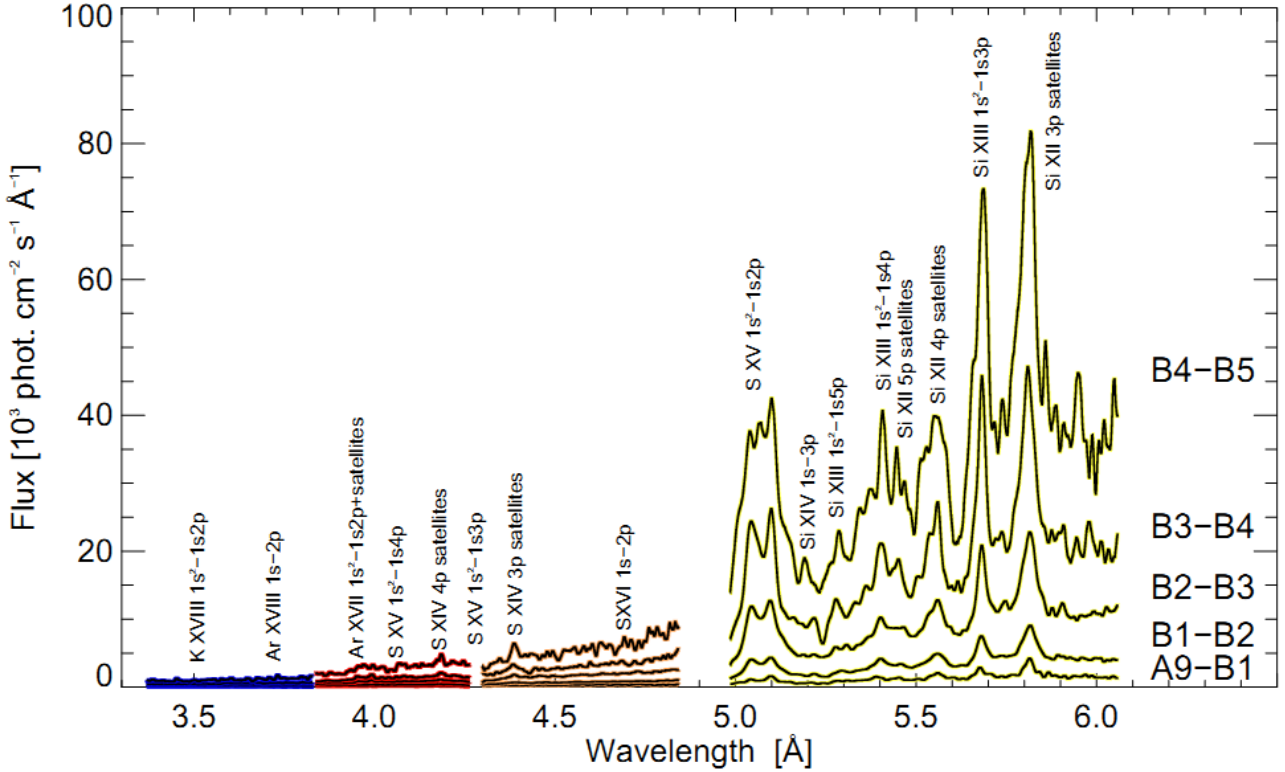

RESIK flare spectra

RESIK/CORONAS-F (2001-2005)

3.5 – 6.1 Å

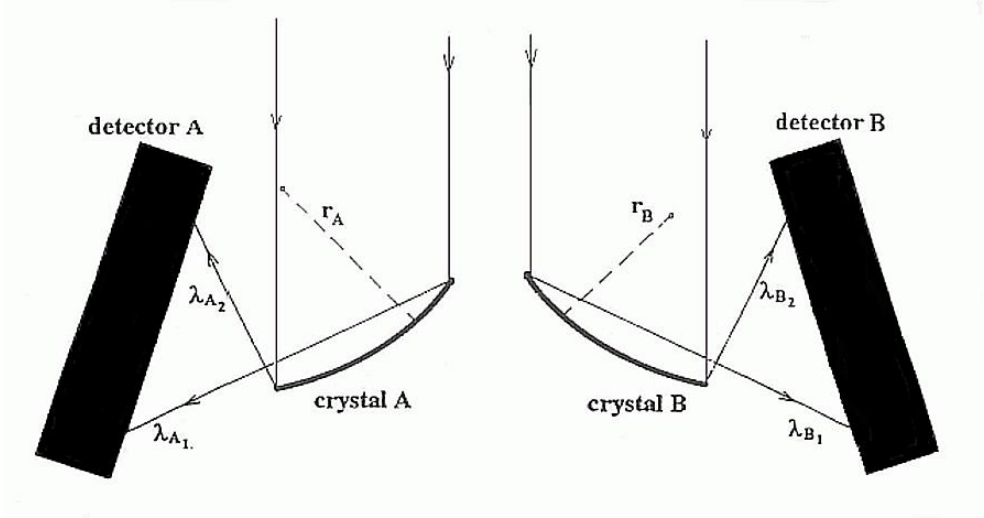

Chifor et al. 2007; C5.8 flare 22 Feb 2003

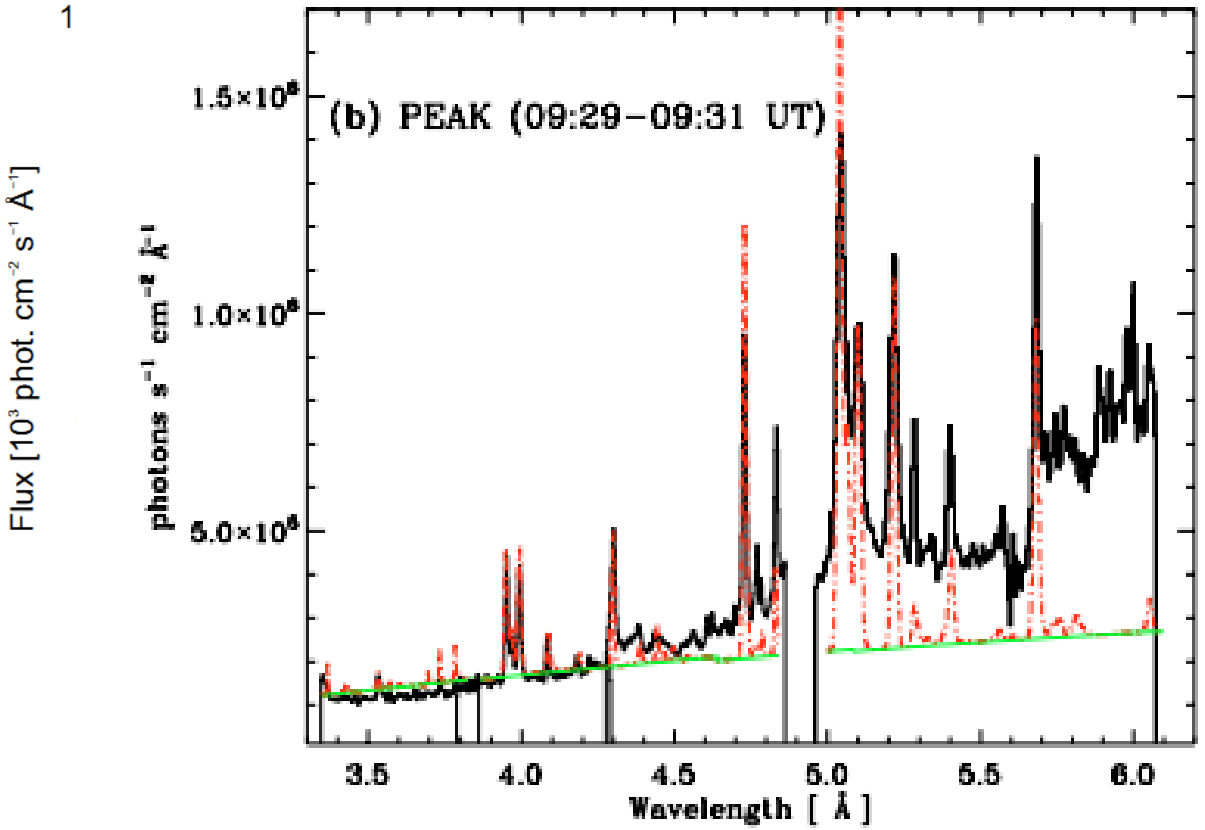

Mg XII spectroheliograph 8.42 Å

Crystal quartz mirror [10 -1 0]

Detector – CCD

2d=8.501 -> Bragg-Wulf -> λ=8.42 Å

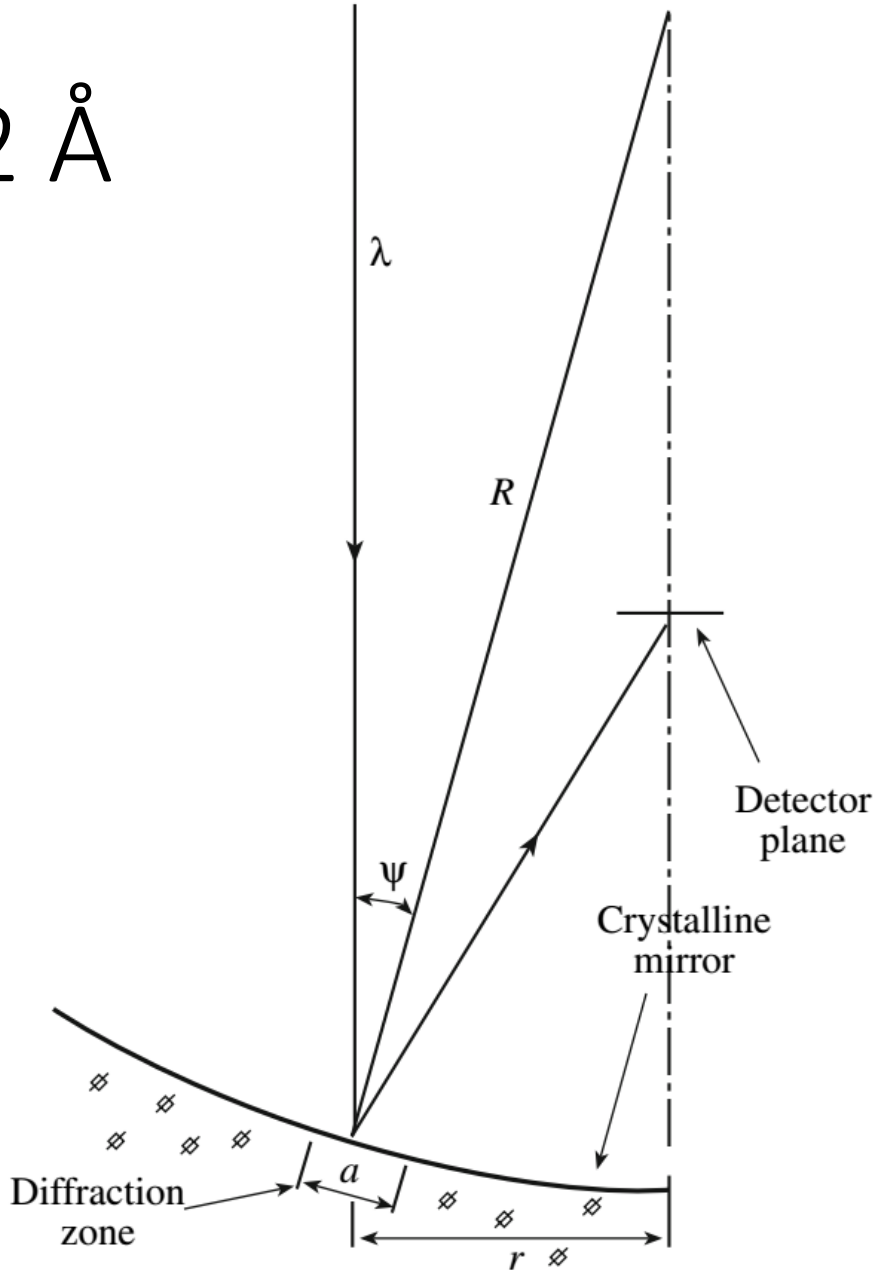

Mg XII spectroheliograph 8.42 Å

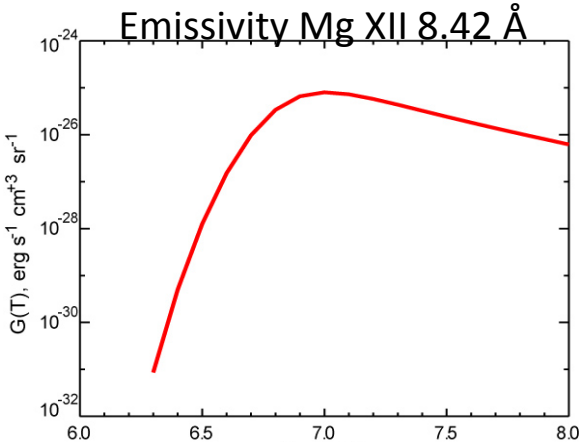

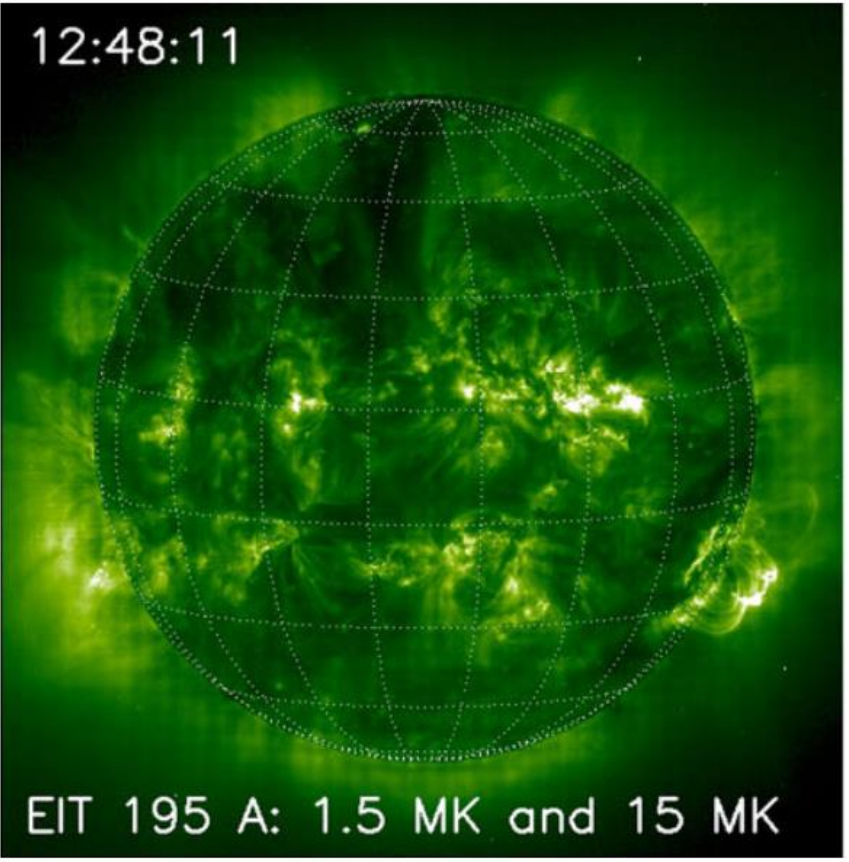

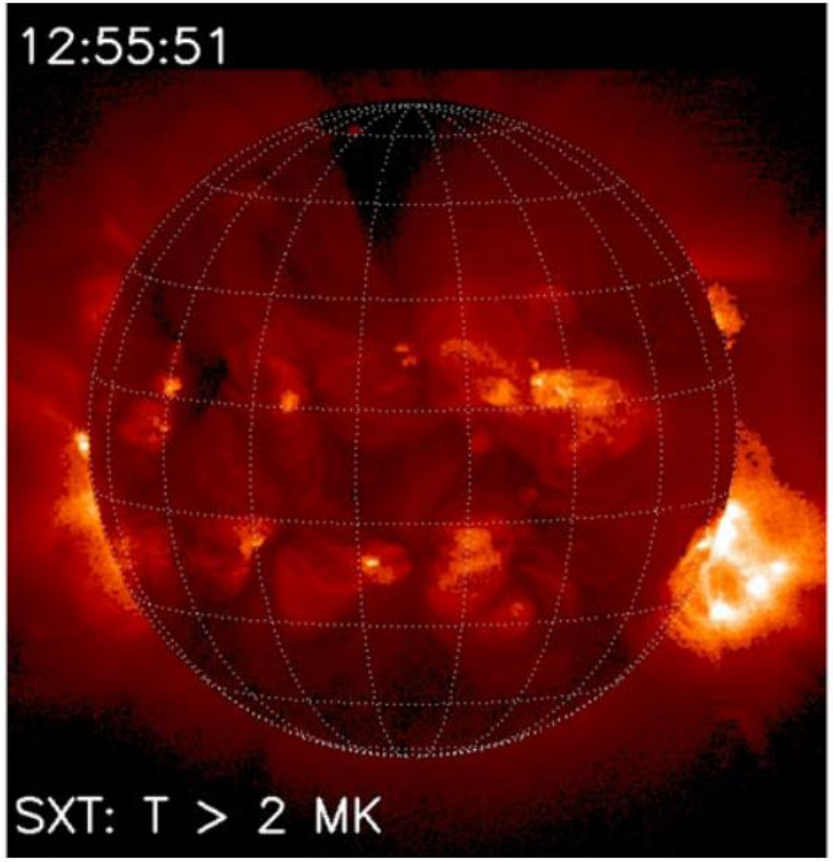

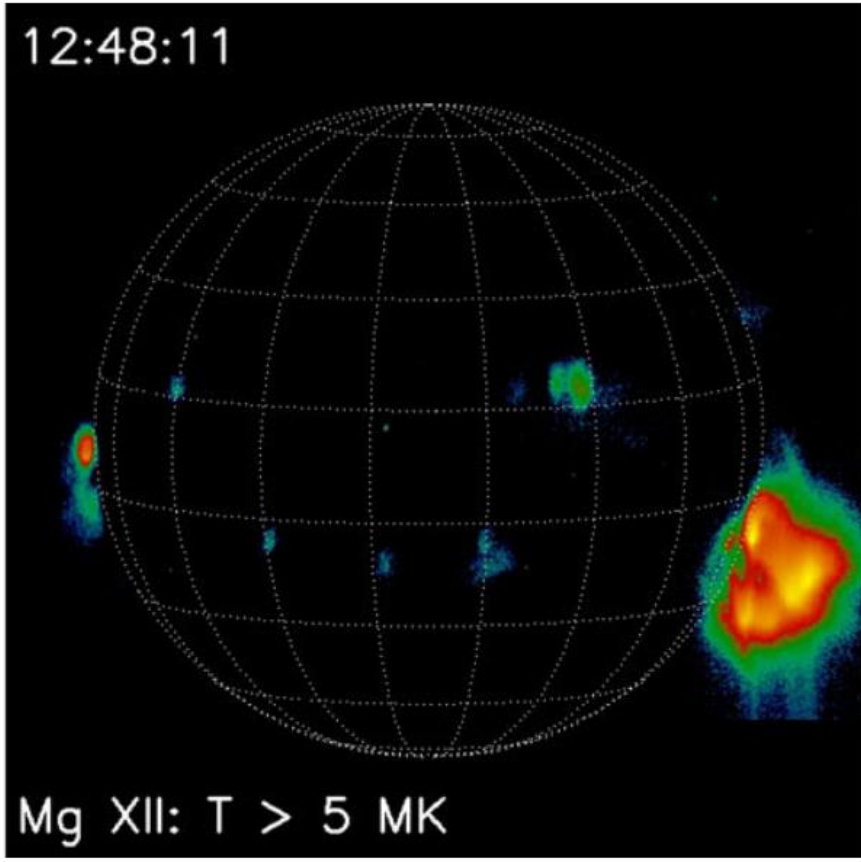

Pros & Cons – crystal spectrographs

- Soft X-ray wavelength;
- Limited set of crystals available;
- Imaging capabilities are limited;
- Really see hot plasma;

Future: **ChemiX** for the InterhelioProbe – SRC, Wroclaw
SolPex for the ISS – SRC&LPI
MaGIXS – from MSFC

MaGIXS spectrograph for Soft X-ray

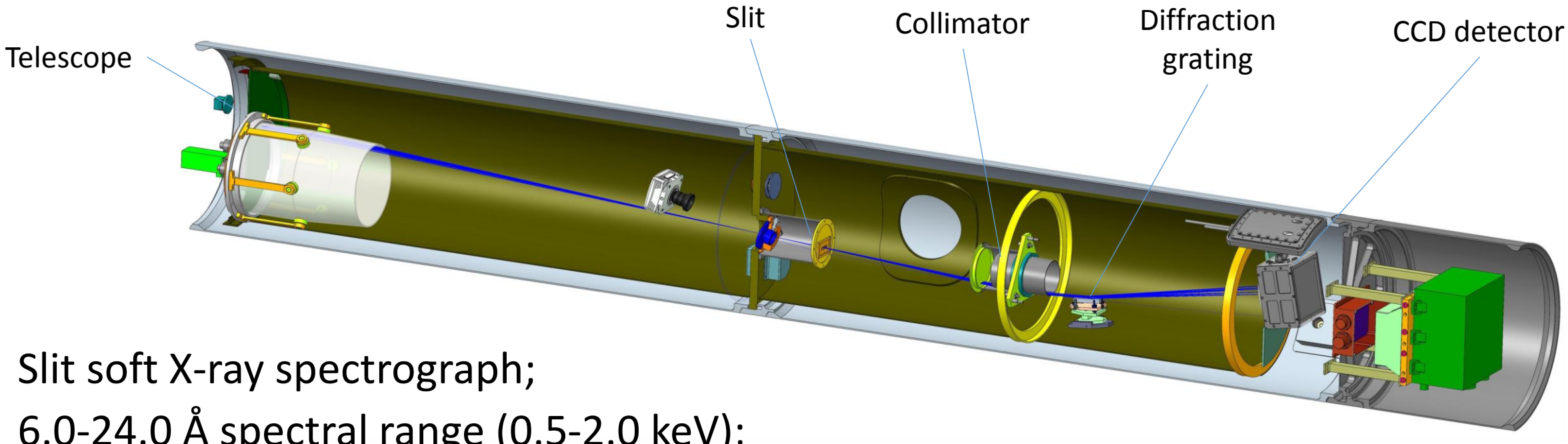

- Slit soft X-ray spectrograph;
- 6.0-24.0 Å spectral range (0.5-2.0 keV);
- Grazing incidence diffraction grating;
- Wolter type I telescope;
- Grazing incidence collimator;
- CCD detector;

MaGIXS – Marshall Grazing Incidence X-ray Spectrometer

Photometers

- Lyra/PROBA-2 - 1200-1230 Å
  - 1900-2200 Å
  - 1-800 Å
  - 1-200 Å;
- GOES SXR detectors - 0.5-4 Å
  - 1-8 Å;

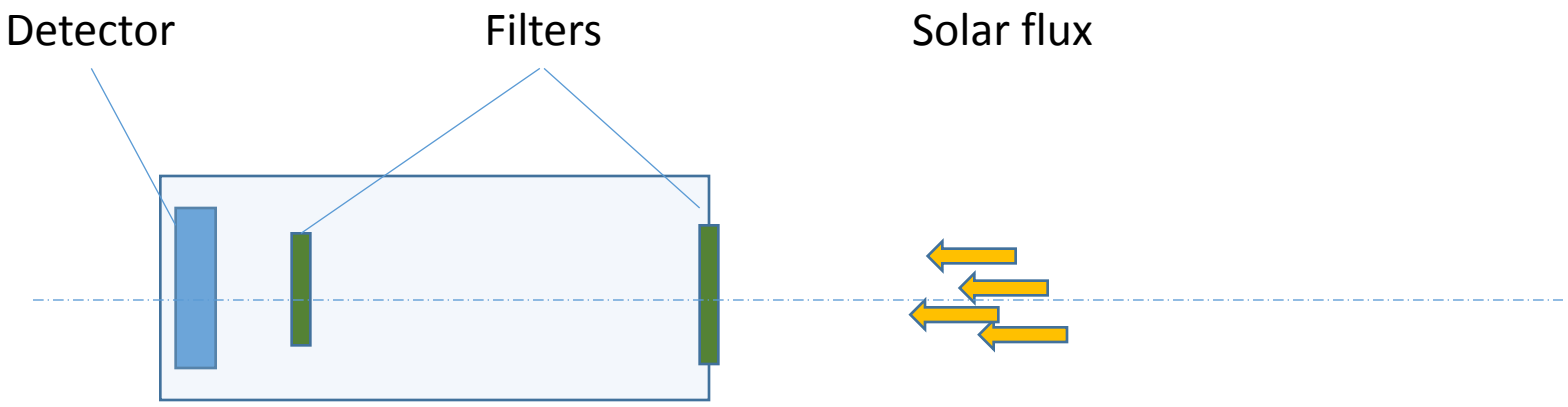

GOES SXR detectors

- Series of satellites since 1974;
- Two ion chamber based SXR detectors;
- Different response of two detectors ->
  Diagnostics of plasma – T, EM

(White et al. 2005)

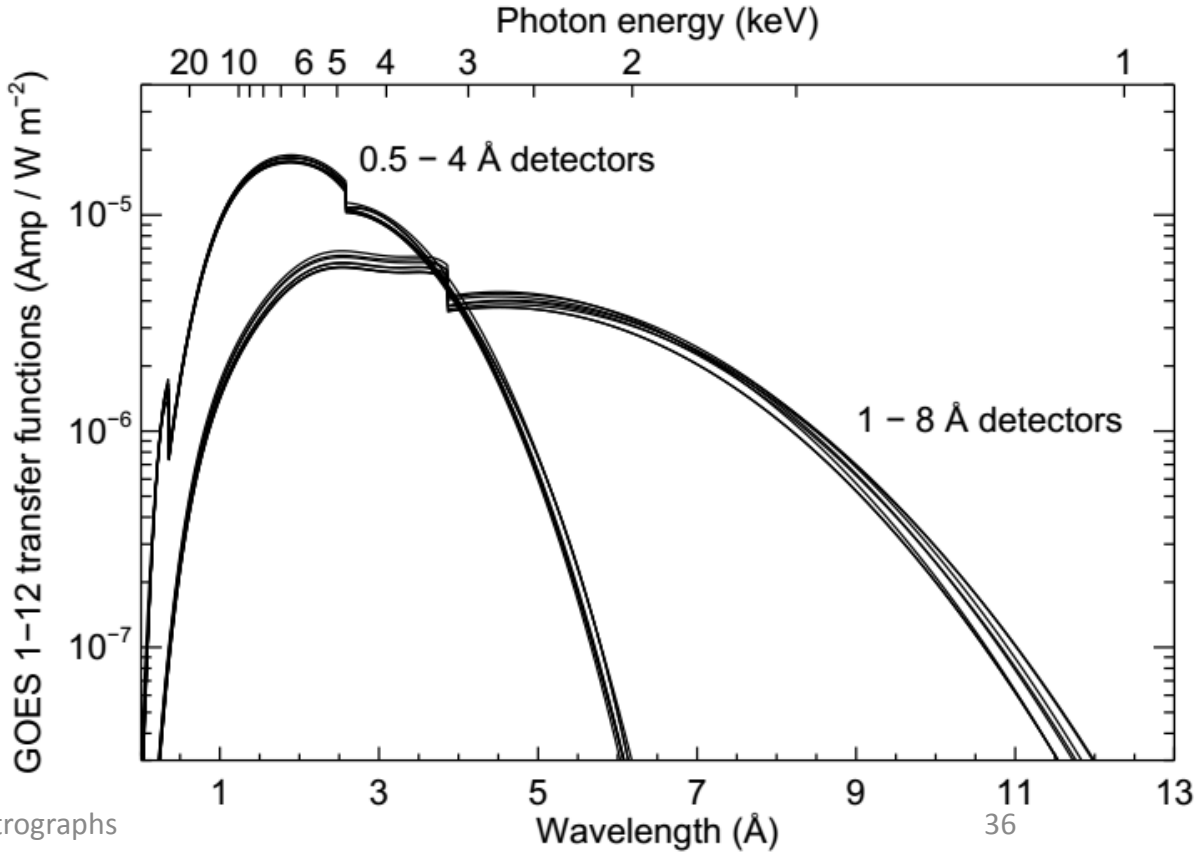

Pros & Cons - photometers

- Relatively simple to build;
- Relatively difficult to interpret data,

  due to registering of “average” signal in “some” passband;

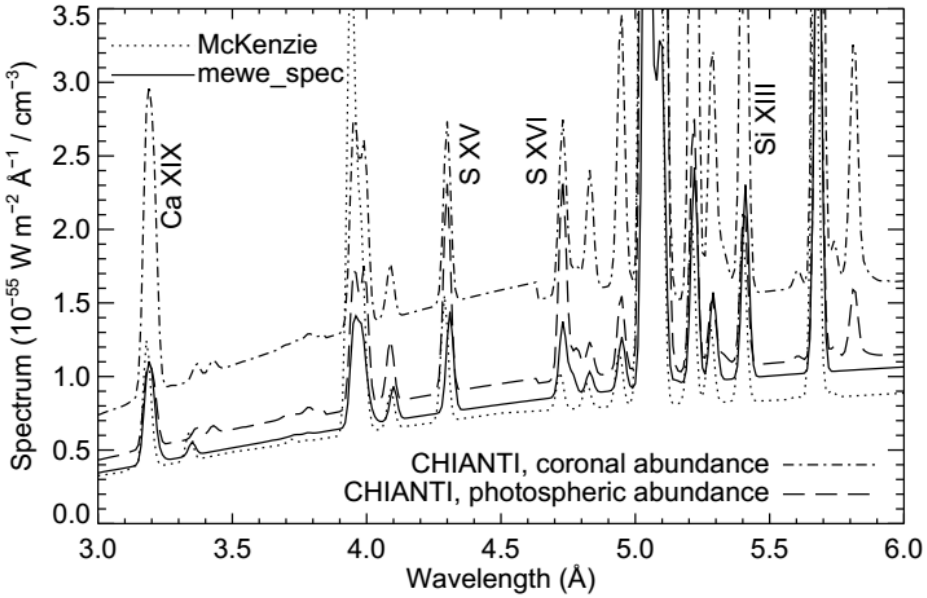

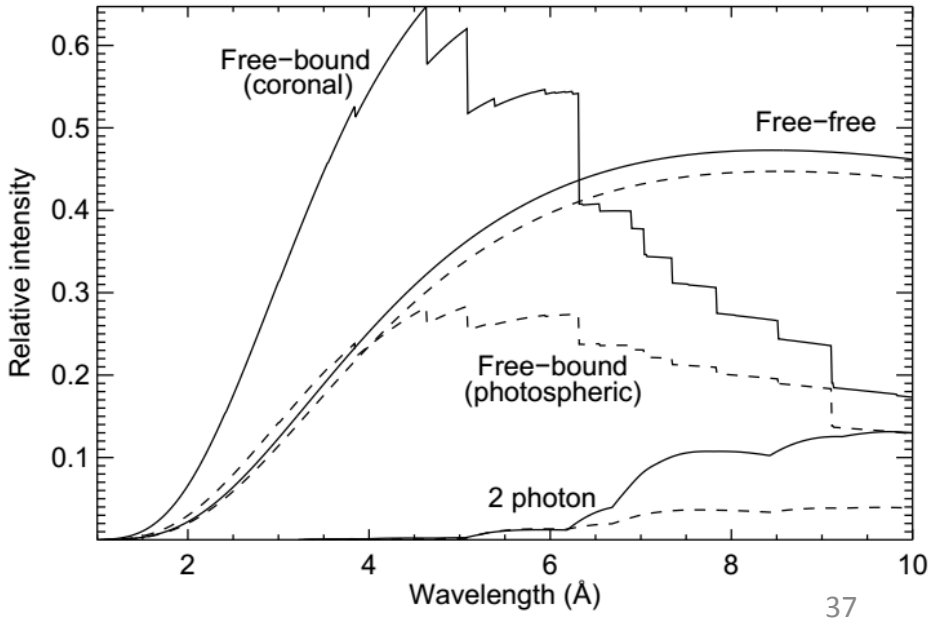

Solid state spectrographs

- Due to absorption in semi-conductor a photon creates charge in the valence zone;
- For Si – 3.6 eV per e-h pair, e.g. 8.42 Å = 1.47 keV -> 410 e^-

- SphinX/CORONAS-PHOTON – Si photodiodes, 0.5-15 keV
- RHESSI – Ge detectors, 4-320 keV;
- SOXT – 4-25 keV Si, 4-56 CdZnTe;
- STIX/Sol.Orb. – CdTe detectors, 4-150 keV

SphinX soft X-ray spectrometer

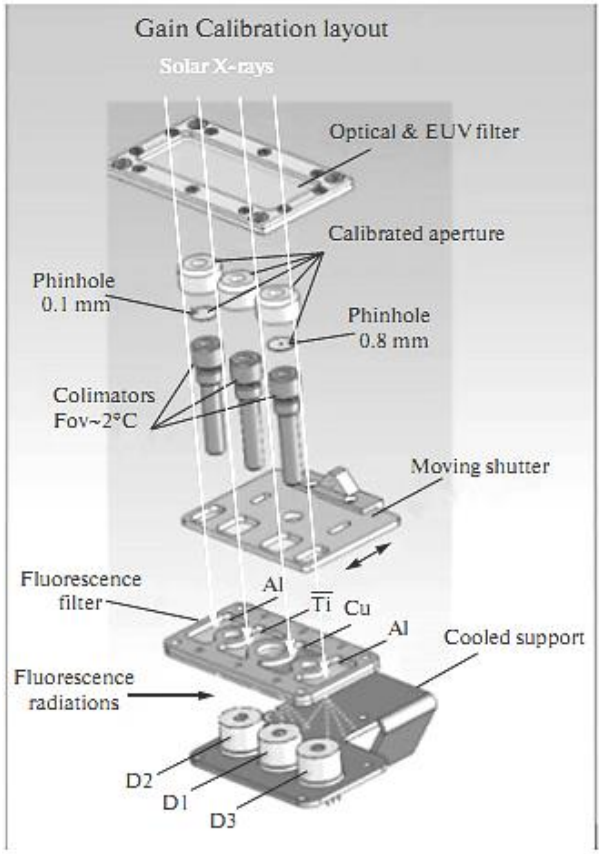

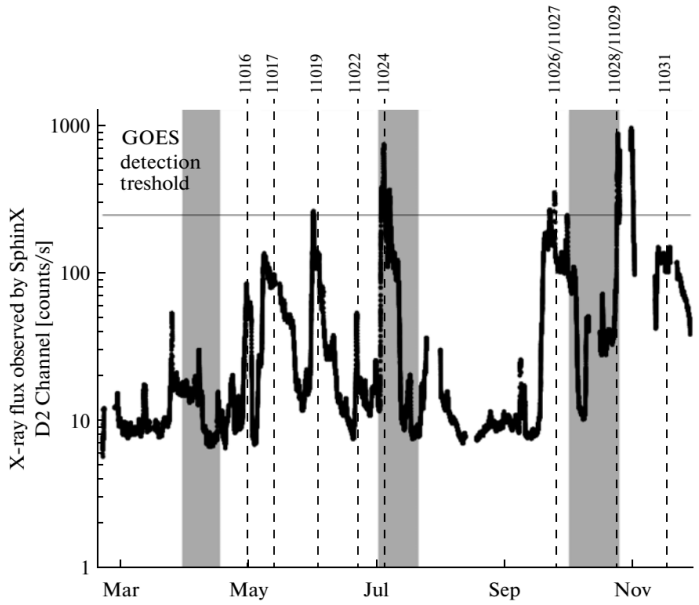

XRT/Hinode

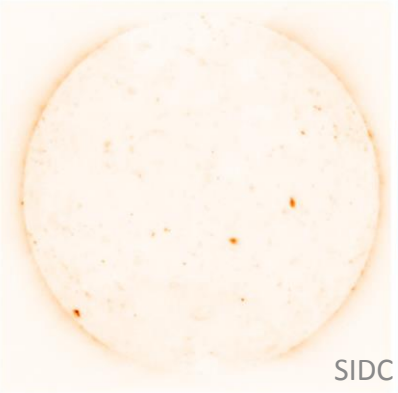

TESIS/CORONAS-PHOTON

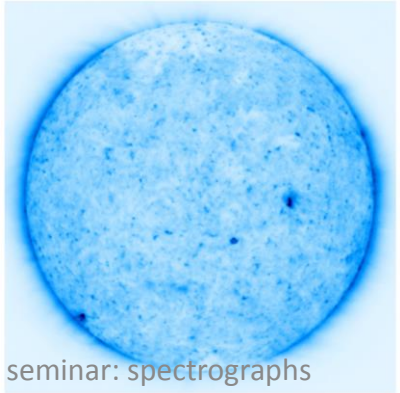

SphinX/CORONAS-PHOTON

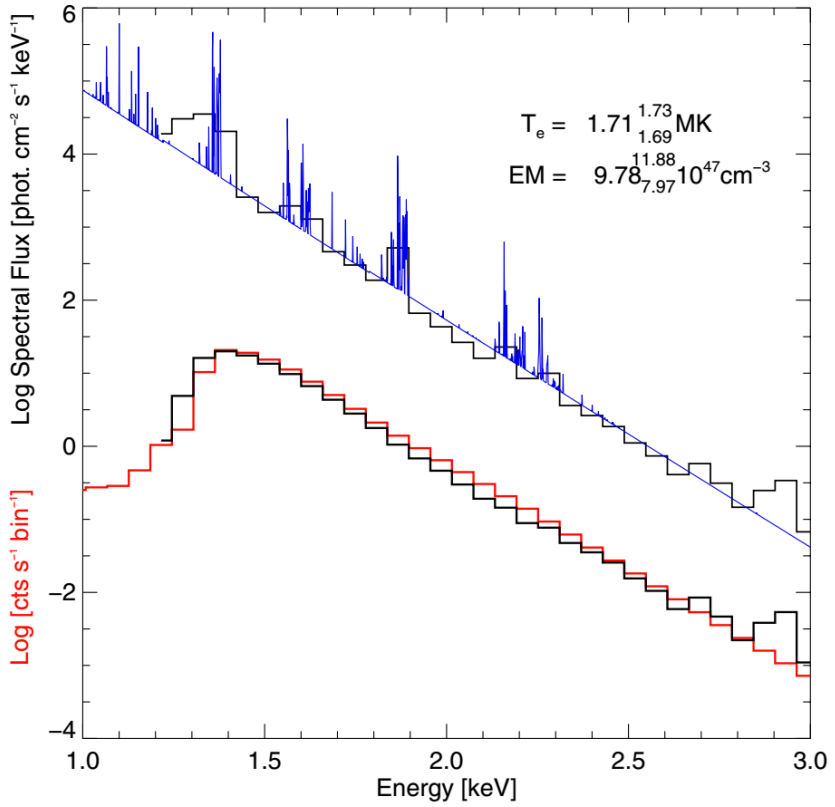

RHESSI

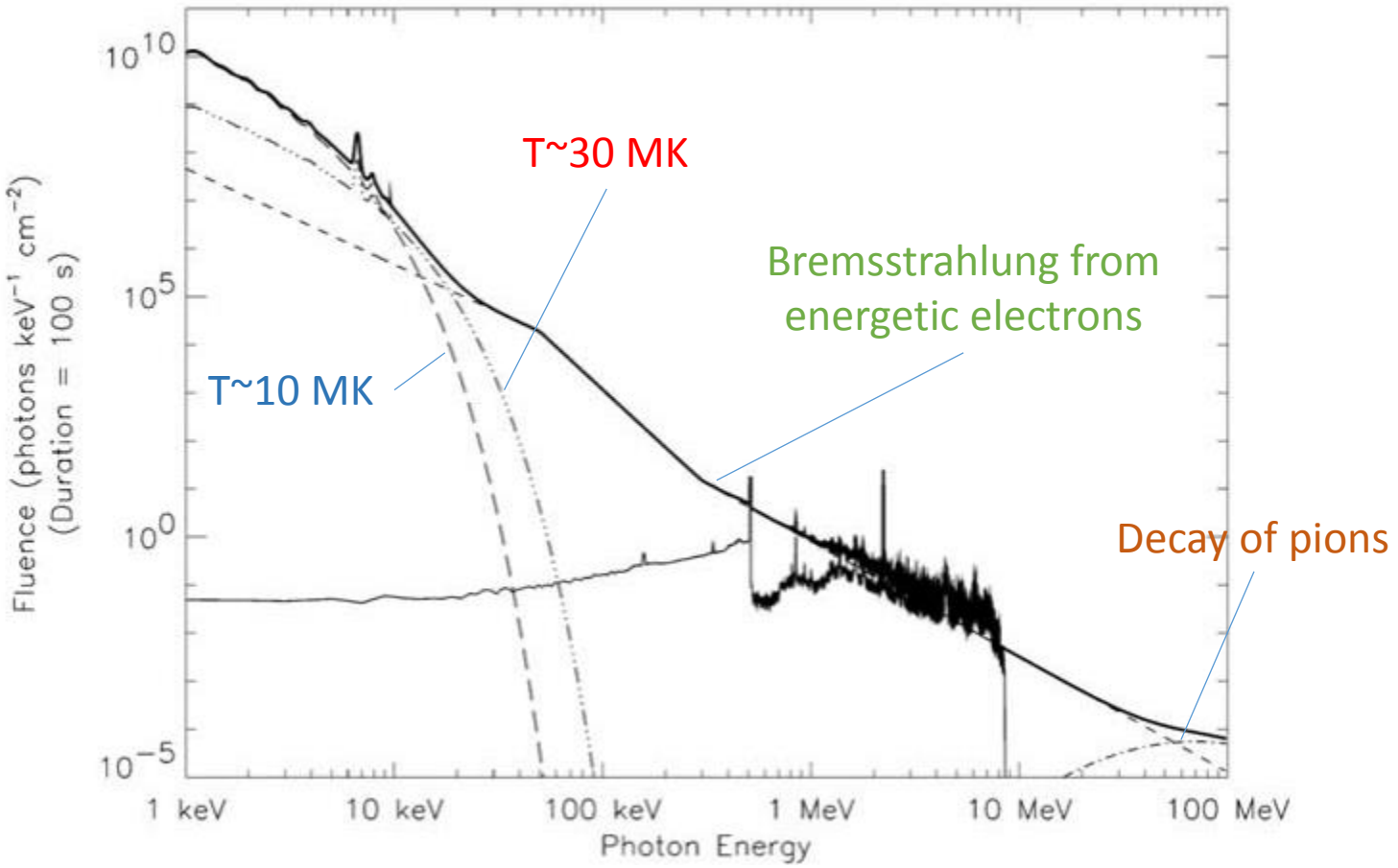

Figure 1. Composite X-ray/gamma-ray spectrum from 1 keV to 100 MeV for a large flare. At energies up to ~ 10–30 keV, emission from hot(~ 10^7 K) and 'superhot' (~ 3×10^7 K) thermal flare plasmas (the *two curves at the left*) dominate. Bremsstrahlung emission from energetic electrons produces the X-ray/gamma-ray continuum (*straight lines*) up to tens of MeV. Broad and narrow gamma-ray lines from nuclear interactions of energetic ions sometimes dominate the spectrum between ~ 1 to 7 MeV. Above a few tens of MeV the photons produced by the decay of pions (*curve at the right*) dominates. RHESSI observations cover almost four orders of magnitude in energy (3 keV to 17 MeV).

Pros & Cons – solid state spectorgraphs

- Possibility to go to higher energies;
- High cadence;

- No spatial resolution?
- Low spectral resolution;

Thank you!

Literature

- K. Phillips, U. Feldman, E. Landi “Ultraviolet and X-ray Spectroscopy of the Solar Atmosphere”
- Doschek, G. A., & Feldman, U. (2010). The solar UV–x-ray spectrum from 1.5 to 2000 Å
- CHIANTI atomic database documentation
- M. J. Aschwanden, “Physics of the Solar Corona. An Introduction” Chapter 2
- Mason, H. E., & Monsignori Fossi, B. C. (1994). “Spectroscopic diagnostics in the VUV for solar and stellar plasmas”

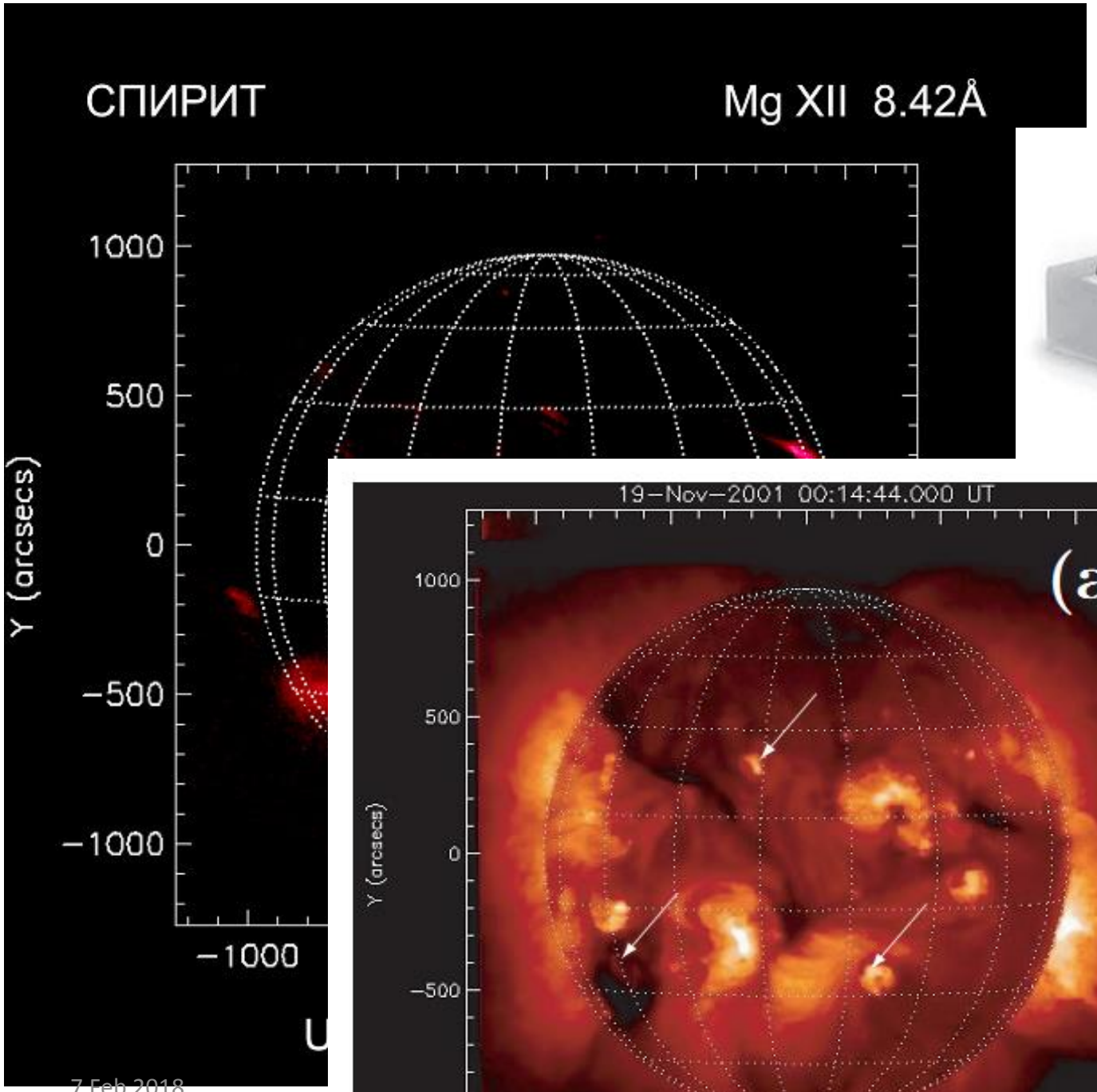
СПИРИТ
Mg XII 8.42Å
1000
500
0
−500
−1000
Y (arcsecs)
−1000

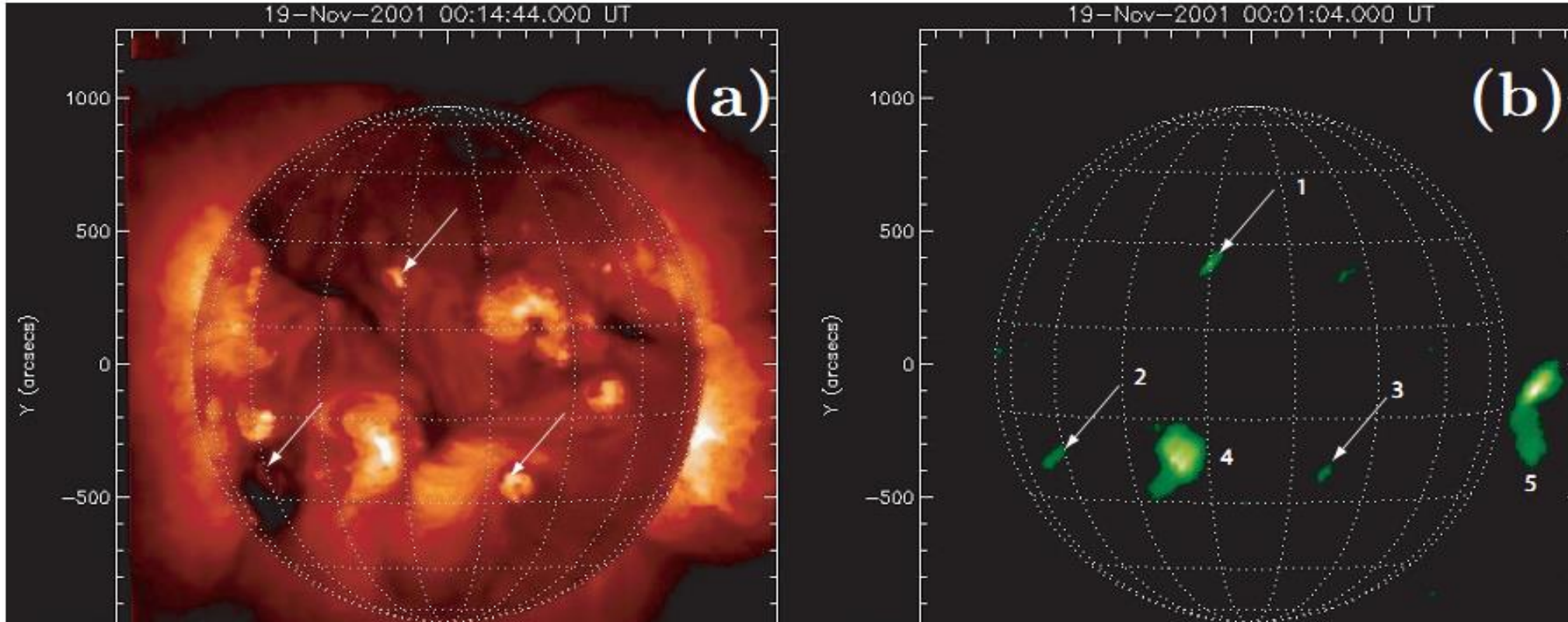
19−Nov−2001 00:14:44.000 UT
(a)
19−Nov−2001 00:01:04.000 UT
(b)
1000
500
0
−500
Y (arcsecs)
1
2
3
4
5

Table 1 EVE solar irradiance instruments. $\Delta\lambda$ is the spectral resolution, Δt is the normal operations integration time (cadence), R is the grating radius of curvature, d is the grating line spacing, α is the grating incidence angle, β is the grating diffraction angle, 1 and 2 for MEGS-B refer to its two different gratings, 2nd is the filter used for second- (and higher-) order sorting calibrations, BI is Back-Illuminated (back-thinned) for the CCD type, AXUV is XUV grade (n-on-p) Si photodiodes from IRD.

Instrument (slit, mm^2)	λ Range (nm)	$\Delta\lambda$ (nm)	Δt (sec)	Filters	Grating	Detector	Description
MEGS-A					$R = 600$ mm	1024 × 2048	Grazing Incidence, Off-Rowland Circle Spectrograph. Grating and Detector are shared with both slits and SAM.
Slit A1	5 – 18	0.1	10	Zr/C	$d = 1304$ nm	BI CCD	
(0.02 × 2)				2nd: Zr/Si/C	$\alpha = 80°$		
Slit A2	17 – 37	0.1	10	Al/Ge/C	$\beta = 73 – 79°$		
(0.02 × 2)				2nd: Al/Mg/C			
MEGS-B	35 – 105	0.1	10	None	$R_1 = 200$ mm	1024 × 2048	Normal Incidence, Double-Pass, Cross-Dispersing Rowland Circle Spectrograph. Entrance Slit and First Grating are shared with MEGS-P.
(0.035 × 3.5)				2nd: Al/Mg/C	$d_1 = 1111$ nm	BI CCD	
					$\alpha_1 = 1.8°$		
					$\beta_1 = 4 – 7°$		
					$R_2 = 200$ mm		
					$d_2 = 467$ nm		
					$\alpha_2 = 14°$		
					$\beta_2 = 19 – 28°$		
MEGS-SAM					None	1024 × 2048	Pinhole Camera.
(26 µm Dia.)	250	80	10	Acton 250W		BI CCD	X-ray Photon Counting.
	1 – 7	1	10	Al/Ti/C			Uses one corner of MEGS-A CCD.

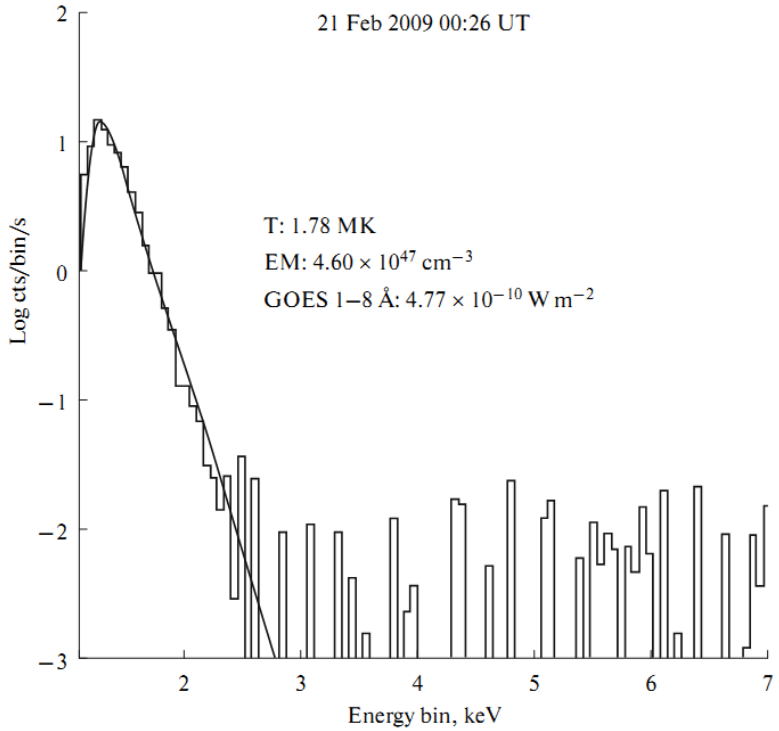
21 Feb 2009 00:26 UT
T: 1.78 MK
EM: 4.60 × 10^47 cm^−3
GOES 1–8 Å: 4.77 × 10^−10 W m^−2
Log cts/bin/s
Energy bin, keV
2
1
0
−1
−2
−3
2
3
4
5
6
7

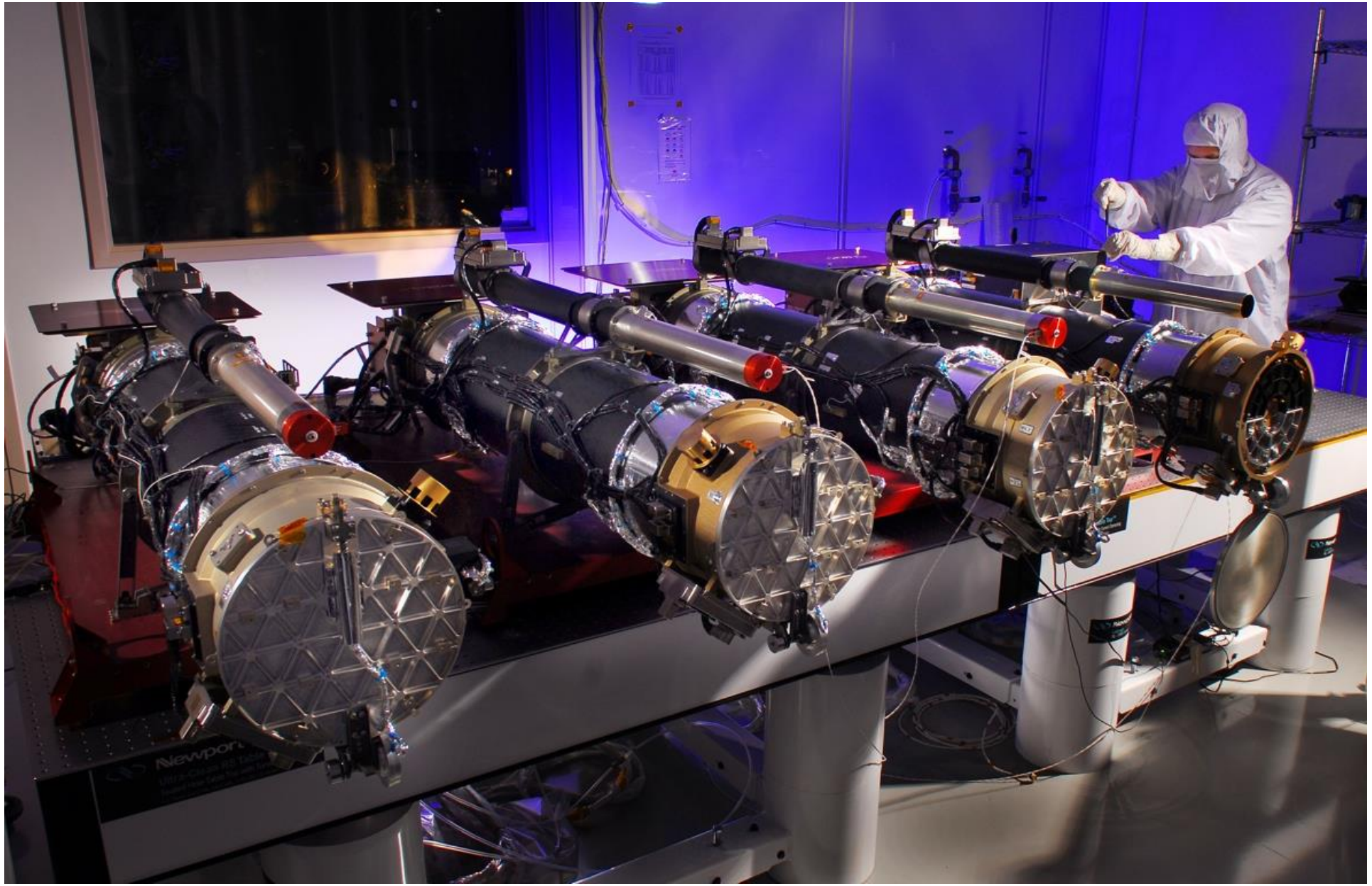

AIA channels and companions: HMI, EIS

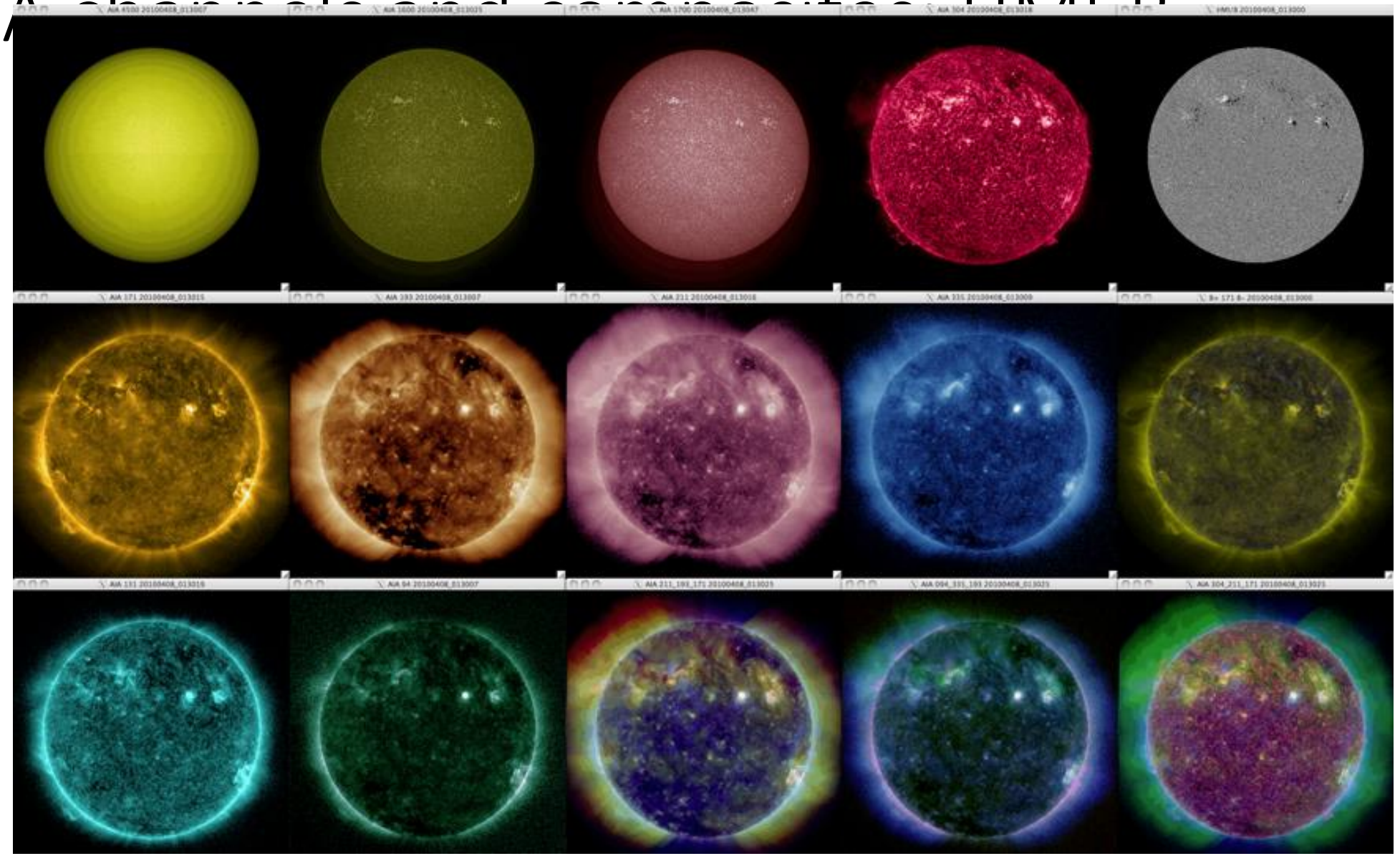

AI

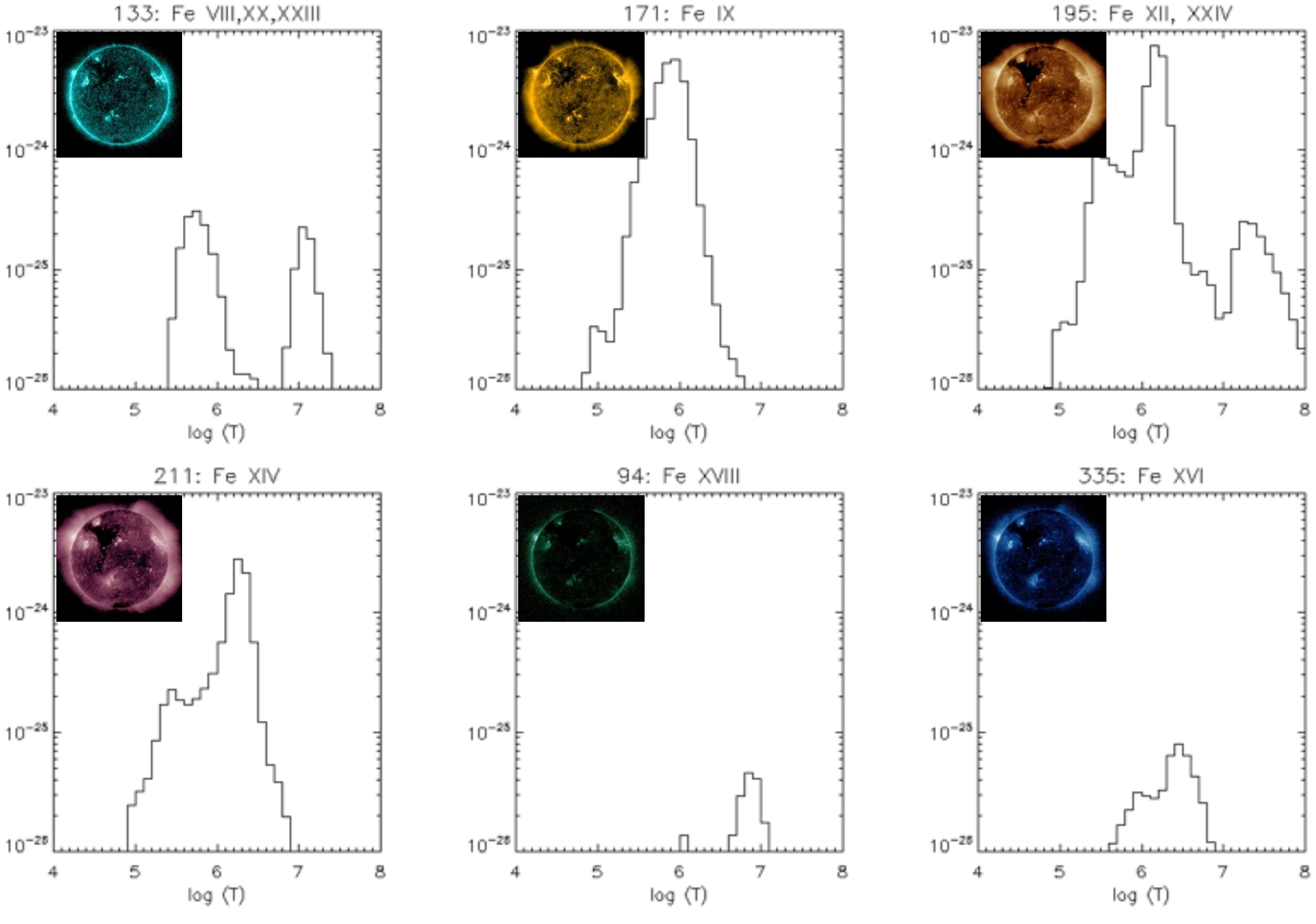
133: Fe VIII,XX,XXIII
171: Fe IX
195: Fe XII, XXIV
211: Fe XIV
94: Fe XVIII
335: Fe XVI
log (T)

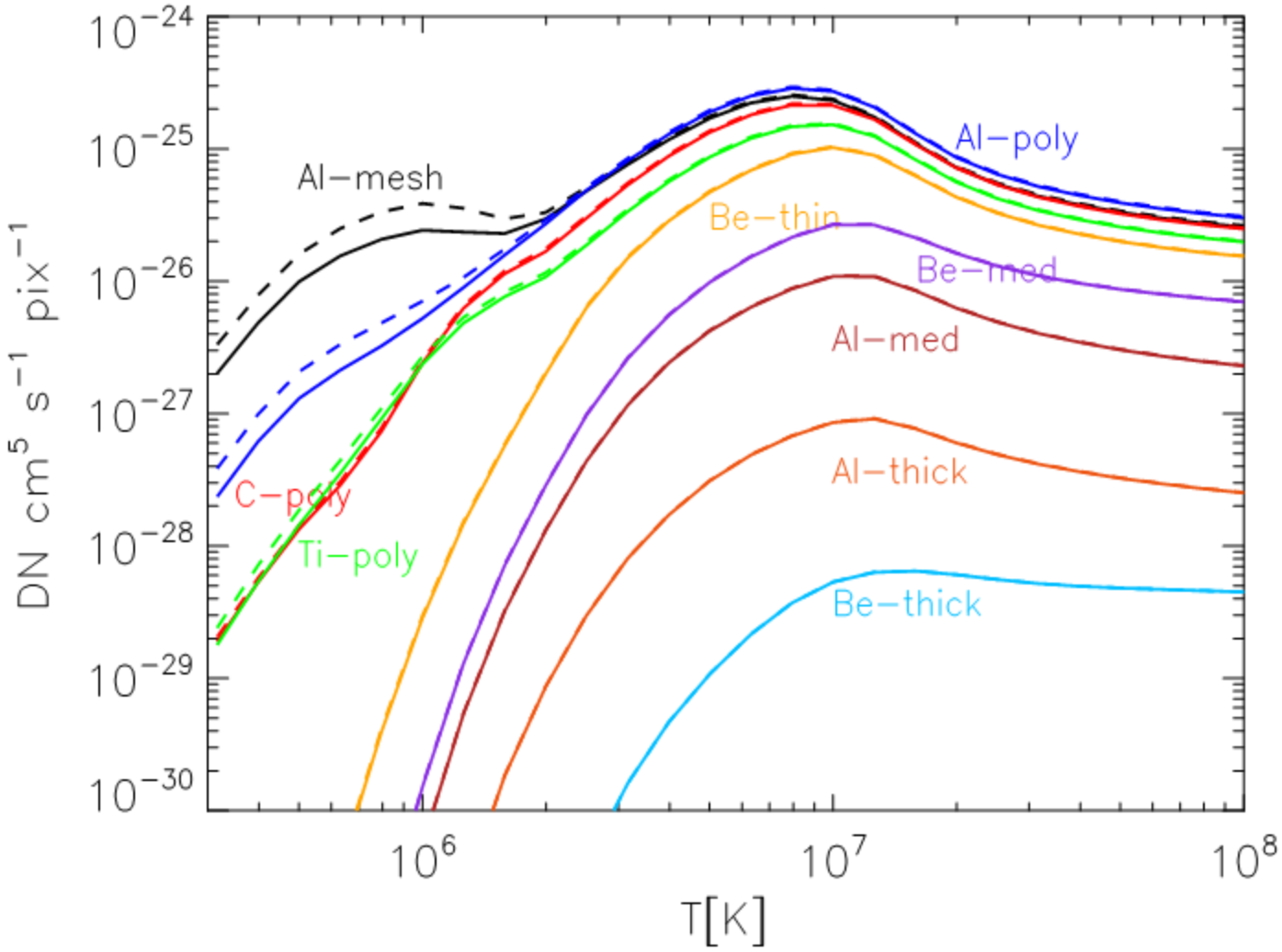
Al−poly
Al−mesh
Be−thin
Be−med
Al−med
Al−thick
C−poly
Ti−poly
Be−thick
DN cm^5 s^{-1} pix^{-1}
T[K]
10^{-24}
10^{-25}
10^{-26}
10^{-27}
10^{-28}
10^{-29}
10^{-30}
10^6
10^7
10^8

High-temperature, low-emission plasma

Random heating of strands can make the loop's intensity appear steady regardless of dynamic heating along one strand.

Discriminator between high-[waves] **and low-**[nanoflares] **frequency heating:**

Relative amount of high-T (5-10 MK) **to average-T** (~3-5 MK) **plasma.**

Blind spot for high-T, low-emission measure using *Hinode*'s XRT and EIS, so ***relative*** amounts of these plasma populations are not accurately known.

MaGIXS will be able to definitively detect and quantify high-temperature, low-emission-measure plasma in the active region core.

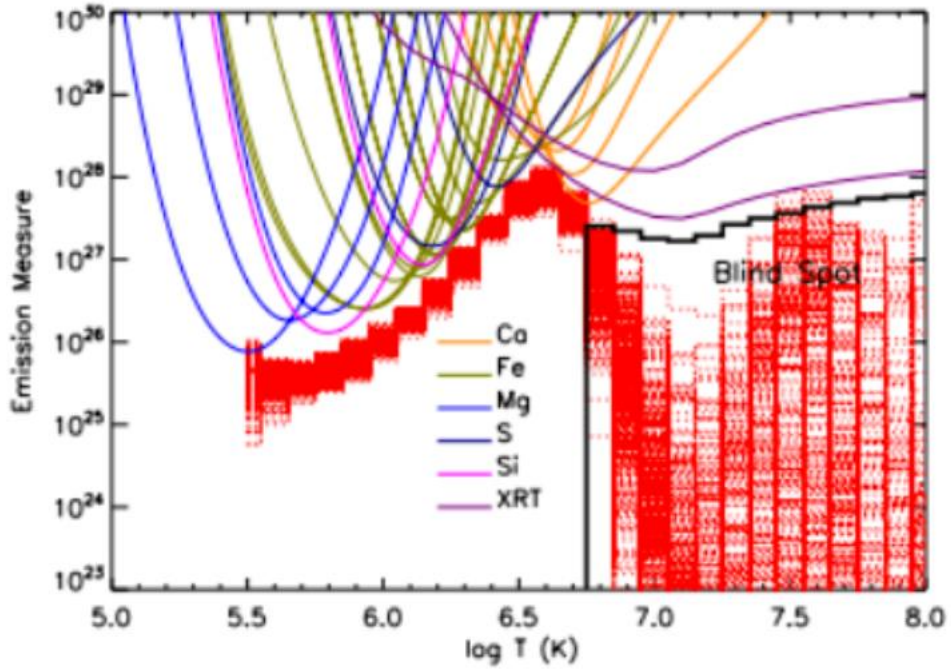

X-ray Solar Flare Spectra